Myosin learns to walk

Amit Mehta

Howard Hughes Medical Institute and Laboratory of Sensory Neuroscience, The Rockefeller University, 1230 York Avenue, New York, NY 10021-6399, USA

(e-mail: mehtaa@rockvax.rockefeller.edu)

Journal of Cell Science 114, 1981-1998 (2001) © The Company of Biologists Ltd

Summary

Recent experiments, drawing upon single-molecule, solution kinetic and structural techniques, have clarified our mechanistic understanding of class V myosins. The findings of the past two years can be summarized as follows: (1) Myosin V is a highly efficient processive motor, surpassing even conventional kinesin in the distance that individual molecules can traverse. (2) The kinetic scheme underlying ATP turnover resembles those of myosins I and II but with rate constants tuned to favor strong binding to actin. ADP release precedes dissociation from actin and is rate-limiting in the cycle. (3) Myosin V walks in strides averaging ~36 nm, the long pitch pseudo-repeat of the actin helix, each step coupled to a single ATP hydrolysis. Such a unitary displacement, the largest molecular step size measured to date, is required for a processive myosin motor to follow a linear trajectory along a helical actin track.

Key words: Myosin V, Single-molecule mechanics, Solution kinetics, Load-dependent kinetics, Structure, Molecular models

Introduction

Managing DNA processing and subcellular transport over micrometers requires motor enzymes that will not leave their tracks before completing tasks. To this end, processive enzymes, such as DNA polymerases and helicases undergo many productive catalytic cycles per diffusional encounter with their binding partners (Lohman et al., 1998). Microtubule motors behave likewise (Howard et al., 1989; Block et al., 1990; Vale et al., 1996): a single conventional kinesin molecule can move along isolated microtubules for hundreds of 8-nm steps (Svoboda et al., 1993), each coupled tightly to an ATP hydrolysis (Schnitzer and Block, 1997; Hua et al., 1997; Kojima et al., 1997; Coy et al., 1999a; Iwatani et al., 1999), before dissociating.

Perhaps as a result of history and circumstance, processivity was long assumed to exclude the myosin superfamily of actin-based motors. A few clues, however, had long fueled speculation regarding class V myosins (Titus, 1997; Howard, 1997). Myosin V purified from chick brain consists of two heavy chains, each with an N-terminal motor domain, a neck region, a tail containing a proximal coiled coil, and a C-terminal globular domain (Cheney et al., 1993) presumed to bind cargo and/or specify subcellular localization (Wu et al., 1998; Reck-Peterson et al., 1999). Each ~23-nm neck region consists of six IQ repeats, each bound to calmodulin (CaM) or a related light chain (Espindola et al., 2000). The motor domain of myosin V shares 41% sequence identity with that of the non-processive muscle myosin II (Espreafico et al., 1992). Moreover, myosin V is especially abundant in neurons and constitutes 0.2% of total protein in brain, which makes it as prevalent as conventional kinesin (Cheney et al., 1993).

In contrast to muscle myosin II, myosin V does not self-assemble into oligomers and is believed to operate in small numbers (Titus, 1997; Mermall et al, 1998; Provance and Mercer, 1999; Reck Peterson et al., 2000a; Miller and Sheetz, 2000), behavior for which a processive motor is well suited. However, investigators remained skeptical for two reasons. First, how could the kinetic scheme deciphered for closely related myosins be adapted to sustain the prolonged and perhaps coordinated actin binding that processive movement would demand? Second, since myosin moves along a helical actin track, wouldn't a hypothetical processive myosin with vesicle cargo spiral about this track and become entangled in a dense cytoskeletal mesh?

Demonstration of processive movement

The gliding filament assay (Kron and Spudich, 1986) allows observation of fluorescent polymer tracks moving upon a field of surface-fixed motors. Low densities of muscle myosin II sustained sporadic and slow actin movements (Uyeda et al., 1990; Uyeda et al., 1991), and significantly lower densities of baculovirus-expressed mouse myosin V fragments also supported motility (Wang et al., 2000), but both only in the presence of methylcellulose to restrict actin filament diffusion.

Tissue-purified chick brain myosin V, however, supported actin motility in the absence of methylcellulose (Mehta et al., 1999a) and at motor densities as low as 0.05 molecules/μm^2 (A. M., unpublished). At saturating ATP concentrations, the actin filament velocity was ~300 nm/s at motor densities from 1000 molecules/μm^2 to 2.7 molecules/μm^2 (Mehta et al., 1999a) or even 0.05 molecules/μm^2 (A. M., unpublished). This is consistent with a very high duty ratio (Uyeda et al., 1990; De La Cruz et al., 1999; Moore et al., 2000), the fraction of cycle time spent strongly bound to the track. Under limiting ATP conditions, actin filaments moved faster over motor densities of 2.7 myosin molecules/μm^2 than they did over 54 molecules/μm^2. Exogenous ADP inhibited this gliding speed (below), but several millimolar P_i did not.

At low densities, actin filaments threaded through and swiveled about isolated surface contact points (Fig. 1A; Mehta et al., 1999a; Wang et al., 2000), which is reminiscent of

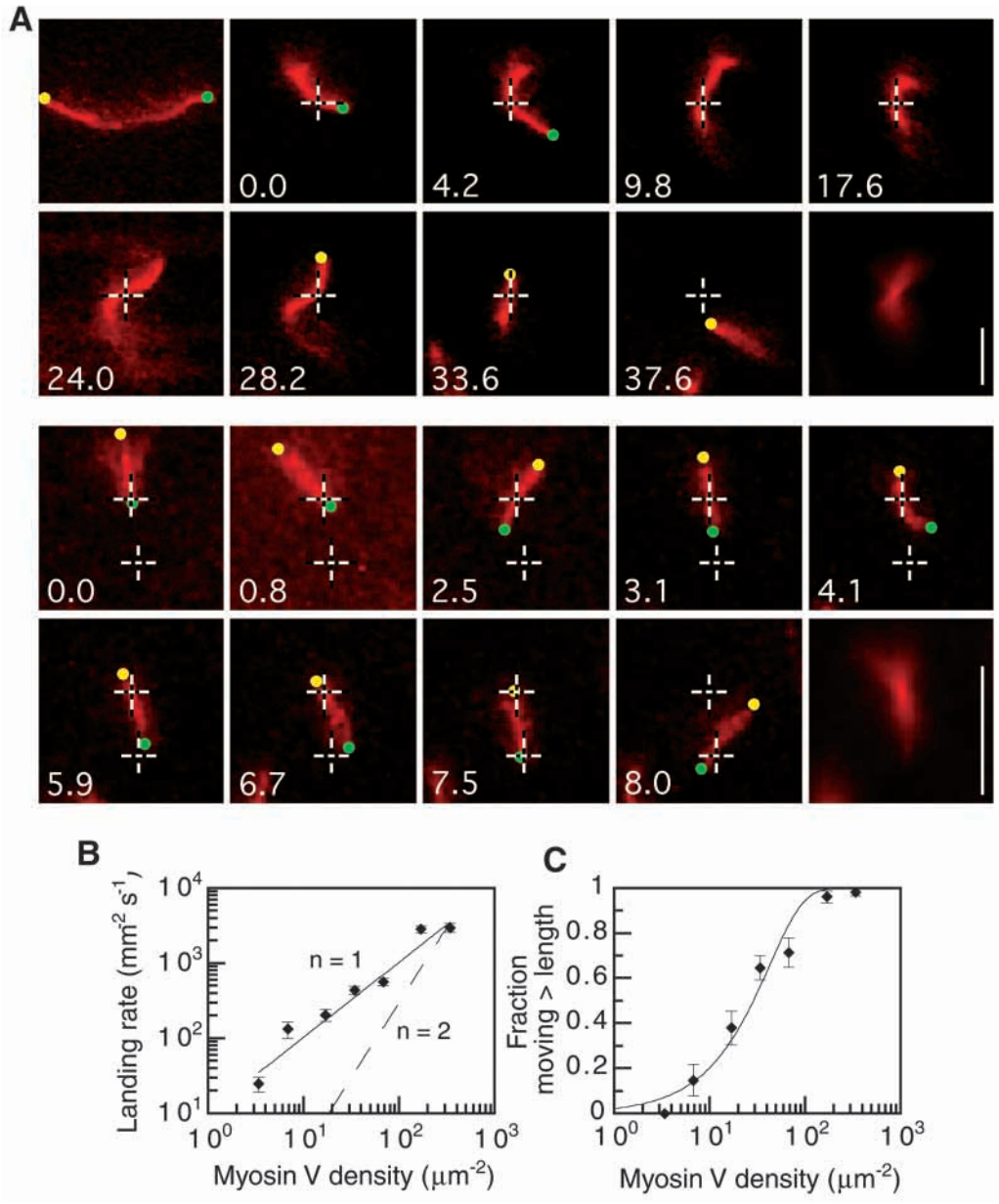

Fig. 1. (A) An actin filament moves over a surface coated with 3.6 myosin V molecules/μm^2 in 2 mM ATP. The pointed (green dots) and barbed (yellow dots) ends of the filament are marked when the ends are in the image plane. Panels 1-10 (left to right) show the time course of a filament before (panel 1) and after (panels 2-9) it has bound the surface. The apparent point of surface contact (crosshair) appears pronounced in the average fluorescent intensity throughout the time course of movement (panel 10). Panels 11-20 show the time course of a shorter filament moving over 5.4 molecules/μm^2. This filament encounters a second contact point before releasing its first. Nodal swiveling behavior reminiscent of seminal observations with kinesin (Howard et al., 1989; Hunt and Howard, 1993) provided the first hint of myosin V processivity (Wang et al., 2000; Mehta et al., 1999a). Bar, 5 μm. (B) The rate at which actin filaments land and move, as a function of myosin V surface density. A filament was considered 'landed' if it moved >0.5 μm and for >2 seconds. (C) The fraction of filaments that moved more than their length (as in panels a11-a20) before dissociating, as a function of surface density. The fit reflects the single molecule model prediction of P(n>1|n>0), where P(N) represents the density-dependent probability that N molecules populate an arbitrary area. Figure reproduced, with permission, from Mehta et al., 1999a (http.//www.nature.com).

microtubules gliding over single kinesin molecules (Howard et al., 1989; Hunt and Howard, 1993). These nodal points may have contained single molecules, several molecules clustered by chance, or aggregates/oligomers that form in solution or on the surface. Gel filtration (Cheney, 1998), equilibrium sedimentation measurements (O. C. Rodriguez and R. E. Cheney, personal communication), images of surface-bound proteins via electron, fluorescence and atomic force microscopy (Cheney et al., 1993; Mehta et al., 1999a; Sakamoto et al., 2000), observations of motility produced by samples depleted of protein by ultracentrifugation (Rock et al., 2000), and kinetic arguments (Howard et al., 1989) excluded both solution oligomerization and surface-induced aggregation.

It remained possible that chance colocalization of more than one molecule was required to support actin motility. To address this possibility, my co-workers and I examined the statistics of filament binding, movement and dissociation over a broad range of surface motor densities (Mehta et al., 1999a). As expected for a processive motor (Howard et al., 1989; Hancock and Howard, 1998), the rate at which filaments landed and moved exhibited first-power dependence on surface protein density (Fig. 1B). However, the power dependence provides only a lower limit on the required number of motors; the same data, at least at the higher densities measured, could be explained if one molecule holds an actin filament near the surface for long enough that others bind and engage. Stronger evidence for processive motility came from observed filament detachment from the surface (Fig. 1C). The fraction of motile filaments that moved beyond their length (Fig. 1A, panels 11-19), measured across several decades of motor density, fit Poisson statistics of P(n>1|n>0), where P(N) represents the density-dependent probability that N molecules populate an arbitrary area (Mehta et al., 1999a). In other words, assume the filament requires x motors to move over an observable distance. If the filament has at least x molecules underneath it

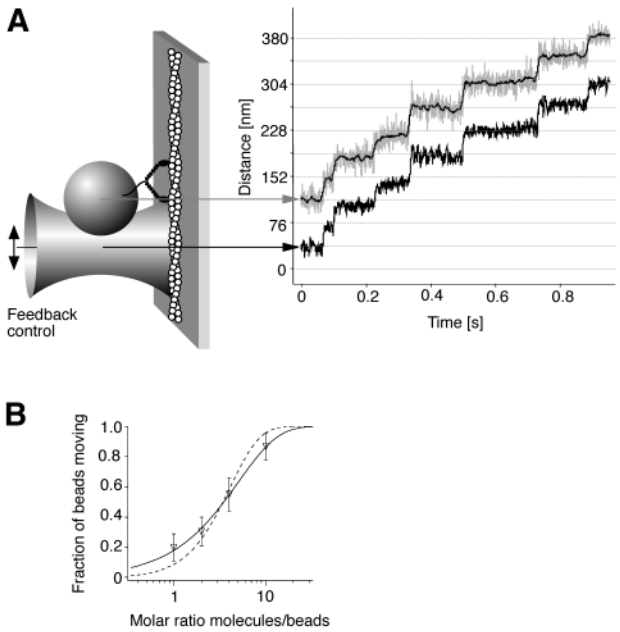

Fig. 2. (A) Illustration of force-clamp records. An optically trapped bead, decorated with myosin V molecules, is moved into close proximity with a surface-mounted actin filament. The bead is subjected to a force-clamp, in which a feedback circuit maintains a constant trap-bead separation and hence constant system tension (left). In some cases, the bead proceeded to step along the actin filament in ~36-nm increments (right) as the trap followed. (B) The fraction of beads observed to step as shown in A, as a function of surface density. The solid line reflects a fit of a single molecule model; the dotted line reflects a model posing two molecules as a minimal agent of such stepping behavior. Reduced χ^2 values for the one- (0.04) and two-molecule (0.98) models rendered relative confidence in the former 25 times that in the latter. Figure reproduced, with permission, from Rief et al., 2000.

- a requirement if the filament is moving - what is the probability of encountering *another* x molecules in the area it sweeps through - a requirement if the filament moving distance exceeds the length of the filament? Such a question generates distinct statistics if x is 1 or 2. Although myosin V and conventional kinesin generate data that fit the single molecule model, Howard and co-workers predicted (Howard et al., 1989; Hancock and Howard, 1998) and observed (Hancock and Howard, 1998) quantitatively distinct behavior from this when a few molecules are required to sustain such motility. From filament movements at very low myosin V density, we inferred that a single molecule can move an actin filament on average more than ~1.6 μm at 25 mM KCl (Mehta et al., 1999a).

To extend these observations, we used optical trapping to observe single molecule interactions at high spatial resolution, employing a dual-bead geometry, in which laser traps capture two beads attached at either end of a single actin filament (Finer et al., 1994; Mehta et al., 1998). The filament is then stretched to tension and moved near surface-bound platforms decorated sparsely with myosin molecules. Under conditions (0.9 molecules/μm^2) where >90% of attempts to solicit molecular binding events failed, most successful attempts resulted in staircase-like displacement records. Isolated binding agents pulled the filament through 3-5-step increments before stalling against 3.0 ± 0.3 pN and dissociating (Mehta et al., 1999a). Might these agents have been multiple molecules? Statistical arguments demonstrate otherwise: on the basis of the low-surface-protein densities (estimated at 0.08 molecules accessible per average attempt) and assuming Poisson statistics govern the distribution of surface motor attachments, the ratio of single to multiple molecule encounters should have exceeded 25. On the basis of the low fraction of observed binding events per solicitation (5-10%), this ratio should have exceeded 20. Whereas the first of these two ratios requires an estimate for the surface contact area sampled in a given attempt, the second relies on no such estimates. Similar observations have been reported for tissue-purified murine myosin V (Veigel et al., 2001).

Later studies used a different experimental geometry (Rief et al., 2000): the motor was attached to polystyrene beads, which were then trapped and moved near surface-mounted tracks (Block et al., 1990; Kuo and Sheetz, 1993; Svoboda et al., 1993). These experiments used a force clamp technique (Visscher and Block, 1998; Visscher et al., 1999), in which a feedback circuit positions the trap to maintain system tension at a programmed level. This scheme prevents motor stalling and dissociation due to prohibitive optical load. At very low motor:bead stoichiometries, we observed beads step throughout the clamp linearity range (Fig. 2A), the position range over which the circuit maintains a constant force, and move for >1 μm when the trap is turned off. The incidence of stepping behavior over a broad range of motor:bead stoichiometries followed single molecule Poisson statistics (Block et al., 1990) and could not accommodate models requiring more than one molecule to support motility (Fig. 2B). Such assays demonstrated that the molecule remains strongly processive even against ~1 pN loads, conditions generally expected to promote more rapid dissociation (Block et al., 1990; Liebler and Huse, 1993). In this experimental geometry, the motor stalled against ~2.5 pN; however, this measurement is less reliable since optical loads are applied both along the axis of movement and perpendicular to it.

Total internal reflection microscopy (Funatsu et al., 1995; Vale et al., 1996) was used to image Cy3-labeled CaM bound to IQ repeats along the neck of tissue-purified chick myosin V (Sakamoto et al., 2000). After confirming that the fluorescent spot intensity distribution of labeled myosin V corresponded statistically with the independently measured Cy3-CaM:myosin-V stochiometry, the authors observed single fluorescent molecules landing upon and moving along single actin filaments (Fig. 3). The run lengths obeyed single exponential statistics - the expected probability of a run length $L \propto e^{-mL}$, where m^{-1} provides the mean length - as expected if release of actin is a stochastic event that exhibits no dependence on past movement. The authors measured a mean run length of 2.4 μm at 150 mM KCl (Sakamoto et al., 2000), which compares favorably with 0.6-1.3 μm kinesin run lengths measured in 0 mM NaCl (Vale et al., 1996; Romberg et al., 1998). Run-lengths for both myosin V and kinesin drop with ionic strength (Vale et al., 1996; Sakamoto et al., 2000).

All of the above experiments involve molecules purified from chick or mouse brain tissue, which - although they bind different light chains (Espindola et al., 2001) and exhibit different kinetic properties (De La Cruz et al., 2000a) - both move processively. By contrast, no processive motility has

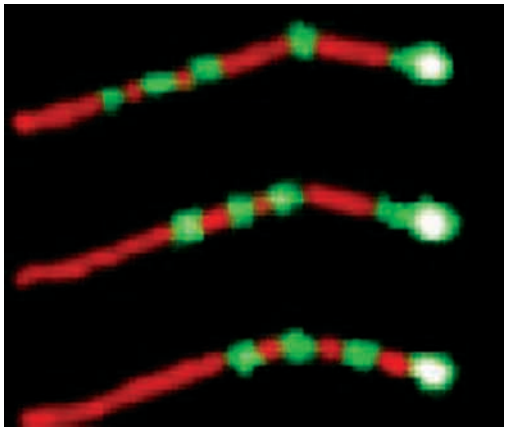

Fig. 3. Single myosin V molecules, imaged by total internal reflection microscopy, move along isolated actin filaments. Myosin V molecules are shown in green; actin is shown in red. Fluorophores appear to accumulate at the barbed filament end. This suggests that, when a single moving myosin V encounters a problem ahead (an absent or occupied binding site), the trailing head remains anchored upon the filament while the leading head remains unbound. Leading head binding may thus induce trailing head dissociation, which is similar to proposed mechanisms for kinesin (Hancock and Howard, 1999). However, uninteresting phenomena, for instance motors moving off the actin filament end and then adhering nonspecifically to the surface substrate, could also underlie observed accumulation. Figure reproduced, with permission, from Sakamoto et al., 2000.

been observed in the dual-bead optical trapping geometry with baculovirus-expressed murine-sequence dimer (HMM) constructs lacking the C-terminal cargo-binding domain (Moore et al., 2001), a region generally assumed to be of little relevance to the N-terminal motor domain. Although these data may derive from problematic surface attachments of truncated motor fragments, it remains possible that complex modes of internal molecular regulation disrupt processivity when the C-terminal domain is removed. Moreover, both *Saccharomyces cerevisiae* myosin V homologs appear to be weakly processive or non-processive (Reck-Peterson et al., 2000b). Although this may derive from kinetic properties of the motors under experimental conditions (see De La Cruz et al., 2000b), it may also illustrate the significance of mechanical, kinetic and functional differences among related members of the same myosin class.

Kinetic requirements for a processive myosin

Decades of solution kinetic experiments have established a basic scheme for ATP turnover by myosin II (Spudich, 1994); the rate-limiting transition involves isomerization from an ADP-P_i state that has a low affinity for actin (weak binding) to an ADP-P_i state that has a high affinity for actin (strong binding; Eqn 1).

$$\begin{array}{ccccccccc} \text{AM} + \text{ATP} & \leftrightarrows & \text{AM-ATP} & \leftrightarrows & \text{AM-ADP-Pi} & \leftrightarrows & \text{AM-ADP} & \leftrightarrows & \text{AM} \\ & & \Updownarrow & & \Updownarrow & & & & \\ & & \text{M-ATP} & \leftrightarrows & \text{M-ADP-Pi} & & & & \end{array} \quad (1)$$

After docking with actin in a strong-binding state, myosin releases P_i and performs mechanical work upon actin. Myosin-ADP remains strongly bound to actin. The transition from strong to weak binding follows the subsequent ADP release and ATP binding. In myosin II, these steps are fast compared with the overall cycle time, itself limited by the transition from weak to strong binding. Whereas the weak-to-strong transition governs the overall cycle time, the strong-to-weak transition governs the rate at which myosin can move actin (Spudich, 1994). Low-duty-ratio motors can move at higher speeds, whereas high-duty-ratio motors can operate in smaller numbers (Howard, 1997). A low-duty-ratio motor can achieve processivity by some means of tethering to or encircling its track (Sakakibara et al., 1999; Okada and Hirokawa, 1999), a tactic probably employed by some DNA enzymes. Without this, processivity demands that the two heads of an intact dimer each have a duty ratio >0.5 to ensure that the molecule remains anchored to the track.

Solution kinetic experiments have demonstrated that monomeric myosin V fragments follow the general scheme of myosin II but that there are key kinetic modifications. In particular, the weak-to-strong transition is not rate limiting and occurs more than ten times faster than the cycling rate (De La Cruz et al., 1999). Moreover, ADP release, regulating the strong-to-weak transition, is the rate-limiting step in the overall cycle (De La Cruz et al., 1999; De La Cruz et al., 2000a, De La Cruz et al., 2000b; Rief et al., 2000). Such measurements indicate that in myosin V the necessary kinetic adaptations to support a high duty ratio have evolved.

Three research groups have characterized baculovirus-expressed monomeric myosin V fragments truncated at the C-terminus after one IQ repeat (De La Cruz et al., 1999, De La Cruz et al., 2000a, De La Cruz et al., 2000b), two IQ repeats (Trybus et al., 1999), or all six IQ repeats (Wang et al., 2000) in the neck. In the remainder of this section, I use 'myosin' to refer to these monomeric myosin V fragments. Measured actin-activated ATP-turnover rates, estimated from time courses of inorganic P_i production, ranged from 3.3 s^{-1} (Trybus et al., 1999; Wang et al., 2000) to 12-15 s^{-1} (De La Cruz et al., 1999) under similar solution conditions. These discrepant numbers subsequently spawned widely disparate conclusions regarding the potential for processive movement, a point to which I will return.

To observe myosin binding to actin, investigators used pyrene-labelled actin, whose fluorescence weakens when myosin binds tightly. In the absence of nucleotide, myosin fragments bound to actin with nanomolar to picomolar affinity (Trybus et al., 1999; De La Cruz et al., 1999) and rates approaching the diffusion limit (De La Cruz et al., 1999). ATP bound actomyosin at ~2-9×10^5 M^{-1} s^{-1} (Trybus et al., 1999; De La Cruz et al., 1999; De La Cruz et al., 2000a; Wang et al., 2000) and dissociated the actomyosin complex at ≥850-870 s^{-1} (Trybus et al., 1999; De La Cruz et al., 1999; De La Cruz et al., 2000a). Hence, in the presence of physiological ATP (mM) concentrations, actomyosin dissociates rapidly compared with steady-state cycling.

To measure the rate of ATP hydrolysis, De La Cruz et al. tracked ADP-P_i formation on fast time scales using quench flow (De La Cruz et al., 1999, De La Cruz et al., 2000a). They observed a 120 s^{-1} burst rate that was limited by ATP binding, followed by a slow rise whose rate depended on the actin concentration. The 120 s^{-1} burst reflects events preceding the initial hydrolysis event and thus provides an underestimate of

the hydrolysis rate. Indirect hydrolysis rate estimates exploited a property shared by many myosins: ATP hydrolysis enhances the intrinsic fluorescence of tryptophan residues in the motor domain. The maximum rate provides an estimate of the ATP hydrolysis rate (Johnson and Taylor, 1978): the sum of the forward and reverse hydrolysis rate constants for myosin V was so measured at 200-800 s^{-1} (Trybus et al., 1999; De La Cruz et al., 1999; De La Cruz et al., 2000b). In the absence of actin, P_i release from the myosin-ADP-P_i state is very slow and rate limiting.

In the presence of actin, the transition from a weak- to a strong-binding myosin-ADP-P_i state limits the rate of cycling by myosins I and II. Myosins limited by this transition will have a low duty ratio, and it is difficult to reconcile such a property with dimer processivity. To observe this transition, De La Cruz et al. mixed myosin with ATP, aged the mixture for 14 ms to allow for ATP binding and hydrolysis, and then added actin and a 'P_i detector' (De La Cruz et al., 1999). They observed a fast phosphate burst that depended linearly on actin concentration; the highest measurement, not yet actin-saturated, was >200 s^{-1}. Because this reflects the transition from weak to strong binding, followed by strong binding to actin and P_i release, it provides an underestimate of the transition rate of weak to strong binding. Since this estimate exceeded all measured steady-state turnover rates by more than an order of magnitude, it excluded the possibility that the weak-to-strong transition or Pi release is rate limiting for actomyosin V cycling.

Myosin-ADP was estimated by pyrene fluorescence observations to bind actin with 6-8 nM affinity (Trybus et al., 1999; De La Cruz et al., 1999). Investigators measured ADP release from actomyosin in three ways. First, a fluorescently modified nucleotide mant-ADP, whose fluorescence increases with myosin binding, allows direct tracking of ADP binding and release. After allowing equilibrium binding of mant-ADP to actomyosin and then flushing with unlabelled ATP, investigators observed a fluorescence increase with rates of 12-16 s^{-1} (De La Cruz et al., 1999; De La Cruz et al., 2000b) and 17-19 s^{-1} (Trybus et al., 1999). Second, pyrene actin can be pre-incubated with myosin-ADP and then flushed with excess ATP. Under these conditions, myosin must release ADP before binding ATP and releasing actin. An observed rate of fluorescence increase slower than the 2-9×10^5 M^{-1} s^{-1} for ATP binding would thus reflect the preceding event, ADP release. A second slow rate was indeed observed and had rates of 13.5-14.5 s^{-1} (Trybus et al., 1999), and 11.5 s^{-1} (Wang et al., 2000). Since this experiment involves a series of three transitions, De La Cruz et al. (De La Cruz et al., 1999) modeled like data using independently measured rates of ADP release and ATP binding, yielding fits consistent with rates of mant-ADP dissociation (above). Third, Trybus et al. pre-incubated actomyosin with ADP, flushed it with excess ATP and monitored subsequent actomyosin dissociation by light scattering (Trybus et al., 1999). This yielded a slow phase of 17-22 s^{-1}, which presumably reflects ADP release.

The above rate estimates broadly agree: ADP release at ~10-20 s^{-1}, rapid dissociation from actin in the presence of ATP, and rapid hydrolysis of ATP. However, the discrepant steady-state cycling rate estimates lead to entirely different conclusions: Trybus et al. and Wang et al. compared their 3.3 s^{-1} cycling rate measurement with a 10-20 s^{-1} ADP-release measurement and concluded that ADP release does not limit the cycle time; rather, they concluded that their myosin V fragments fall short of the 0.5 duty ratio (Trybus et al., 1999; Wang et al., 2000). By contrast, De La Cruz et al. estimated both the cycling rate and ADP release at ~12-17 s^{-1} and concluded that ADP release limits the cycling rate (De La Cruz et al., 1999). They argued that such a high monomer duty ratio could enable the intact dimer to move processively.

The key to this discrepancy may lie in a phenomenon all three labs noted and a theme of growing relevance to myosin enzymologists: high affinity for ADP (De La Cruz et al., 2000b). ADP bound to actoymyosin at 9-15×10^6 M^{-1} s^{-1} (De La Cruz et al., 1999; Wang et al., 2000; De La Cruz et al., 2000a; De La Cruz et al., 2000b), 5-20 times the 0.7-1.6×10^6 M^{-1} s^{-1} ATP-binding rate, and with ten times the affinity of ATP (De La Cruz et al., 1999; Wang et al., 2000). Hence, if ADP accumulates over the several minutes routinely taken in steady-state cycling measurements, it will compete with ATP for binding to actomyosin and thus slow the observed production of P_i. In fact, significant non-linearities appear in the measured P_i production rates (De La Cruz et al., 1999), and attempted fits to linear rates can yield artifactually low turnover-rate estimates from extended time courses. De La Cruz et al. used two methods to circumvent this problem. First, they measured a ~12-15 s^{-1} ATP-turnover rate from heavy data sampling in the brief initial period of turnover, before ADP could accumulate, using steady-state Pi generation and quench flow under saturating actin conditions (De La Cruz et al., 1999). Second, they used an ATP-regeneration system to prevent ADP accumulation (De La Cruz et al., 2000a; De La Cruz et al., 2000b). This provided an independent 12-17 s^{-1} measurement. De La Cruz et al. further demonstrated, using rate constants measured by the three labs, that an attempted cycling rate measurement performed over 20-300 s would yield an observed 2-4 s^{-1} rate (De La Cruz et al., 2000b). Hence, several lines of evidence support the notion that 3.3 s^{-1} measurements had underestimated a 12-14 s^{-1} rate. Moreover, an entirely different experiment, independent of any cycling rate estimate, demonstrated that ADP release limits the rate of chemomechanical cycling by an intact dimer moving on actin.

Single-molecule stepping kinetics and their mechanistic implications

Repeatable solution kinetic measurements of rate constants reflect statistics describing stochastic processes, such as the release of one molecule from a binding partner. A rate constant reflects the probability of an event occurring per unit time. When individual molecules are observed directly, a stochastic process will yield variable measurements. However, large numbers of such measurements give rise to robust distributions, from which one can infer the number and rates of biochemical transitions that limit the rate of the observed event (Schnitzer and Block, 1995). In the case of an individual stepping molecule, the distribution of dwell times (τ) separating discrete steps contains information about the biochemical transitions limiting the rate of mechanical advances (Svoboda et al., 1994; Schnitzer and Block, 1995; Schnitzer and Block, 1997; Hua et al., 1997; Kojima et al., 1997; Visscher et al., 1999).

Such transitions can depend on load in interesting ways (see below), but, for now, note that a molecule moving against elastic load, such as a stationary optical trap or glass fiber, will experience steadily increasing resistance as it further strains the probe. Since each step occurs against a different load, one cannot combine all observed dwell times to generate a meaningful distribution. To circumvent this problem, Rief et al. used a feedback circuit that moved the optical trap so as to clamp the load at a programmed level (Visscher and Block, 1998; Visscher et al., 1999; Rief et al., 2000). Observations in the presence (Rief et al., 2000) or absence (Mehta et al., 1999a) of such feedback indicate that the mean stepping rate (τ^{-1}) under all ATP conditions remains independent of load below 1 pN. Rief et al. thus observed dwell periods under a clamped 1 pN load and under various solution conditions (Rief et al., 2000). We reached three conclusions. (1) The stepping process at 2 mM ATP and negligible ADP concentration can be described by a single, rate-limiting 12.5 s^{-1} transition. (2) The stepping process at 2 mM ATP and 200 μM ADP, where the speed of movement is slowed by 50%, can be described by a single apparent rate-limiting 6.4 s^{-1} transition, which means that ADP release limits the stepping rate. If ADP release were not responsible for the apparent 12.5 s^{-1} transition measured in the absence of exogenous ADP, then one would have instead observed two apparent transitions in series, each of rate ~12.5 s^{-1}, when sufficient ADP was added to slow the speed by 50%. Moreover, the data show that when ADP rebinding slows the cycling rate, the release of post-hydrolysis ADP and the release of rebound ADP must occur at the same rate. (3) The stepping process under varied ATP concentrations gives rise to a single apparent ATP-dependent transition per mechanical step, which has a rate constant of 0.9×10^6 M^{-1} s^{-1}, which compares favorably with the above described $0.7\text{-}1.6\times10^6$ M^{-1} s^{-1} ATP-binding rate measured in solution. These measurements show that mechanical steps against ≤1 pN of resistance remain tightly coupled to ATP hydrolysis events, regardless of ATP concentration. The data exclude scenarios in which one ATP binding event precedes more than one mechanical step or two or more ATP binding events precede each mechanical step. All of the aforementioned observations, of course, pertain to ≤1 pN loads, which do not affect the stepping rate. Distinct behavior occurs when the molecule steps against higher loads, a point to which I now turn.

Linear molecular motors often exhibit strain-sensitive biochemistry. Perhaps the best-known example is the Fenn effect in muscle (Fenn, 1924), the slowing of both heat and work output when a contracting muscle faces successively greater resistance beyond a certain point. This reflects a decrease in the rate of ATP turnover, which is effected by a load-dependent decrease in the rate of crossbridge detachment, when cyclical crossbridge attachments serve mainly to bear tension (see Hibberd and Trentham, 1986). Single-molecule experiments have unearthed several other examples of load-dependent chemistry (Mehta et al., 1999b, Ishii and Yanagida, 2000). (1) Early observations of non-processive binding events by muscle myosin II demonstrated that 4-7 pN loads accelerate actomyosin dissociation at limiting ATP concentrations but decelerate it at saturating ATP concentrations (Finer et al., 1994). While the latter observation is consistent with the Fenn effect in muscle, the former indicates that ATP binding or myosin-ATP dissociation from actin is accelerated by strain. (2) Early observations of kinesin revealed a linear force-velocity curve under all ATP conditions (Svoboda and Block, 1994; Meyhofer and Howard, 1995; Kojima et al., 1997; Coppin et al., 1997; see also Hunt et al., 1994). This implied that K_M^T, the ATP concentration required for turnover at half the maximal rate, does not vary with load (Svoboda and Block, 1994; Meyhofer and Howard, 1995). Controversial interpretations of these data (Howard, 1995) were clarified only after more sophisticated and precise measurements showed the K_M^T indeed increases with load (Visscher et al., 1999), through at least one load-dependent transition rate related to binding ATP or committing it to hydrolysis (Visscher et al., 1999; Schnitzer et al., 2000). (3) Observations of RNA polymerase demonstrated that the transcription rate remains independent of load below ~20 pN (Wang et al., 1998; Davenport et al., 2000) and drops sharply as the load rises above this (Wang et al., 1998). From these data, Wang et al. concluded that load-dependent transitions in the absence of load occur 5×10^4 times faster than load-independent transitions (Wang et al., 1998). Moreover, load affected the cycling rate through a characteristic distance of around 5-bp repeats, which reflects either molecular strain or enzyme slippage along the DNA template in the transcriptionally upstream direction. (4) Recent observations of DNA polymerases reveal quite different behavior: addition of each base in the complementary strand is rate limited by a load-dependent transition, perhaps one from weak to strong binding between the template strand and its growing partner (Wuite et al., 2000; Maier et al., 2000). The associated characteristic distance spans multiple bases on the ssDNA template, indicating that more than one base participates in this transition. Investigators are presently characterizing load-dependent statistical kinetics of the lambda exonuclease (Perkins et al., 2001) and the bacteriophage ϕ29 DNA-packaging motor (Tans et al., 2001).

The above studies of kinesin and DNA-based motors involve motors that have small step lengths (perhaps 0.3 nm for various DNA motors) and/or fast stepping rates (~100 s^{-1} for kinesin) that allow thermal noise to mask the underlying molecular trajectory. Attempts to extract mechanistic information from velocity measurements give rise to difficult and often controversial interpretations (see Howard, 1995), because load can affect such measurements in different ways. For instance, load could affect the chemomechanical coupling efficiency, the incidence of backward slippage, the rate of catalysis, and/or the unitary step distance. Although investigators have advanced conclusions regarding load-dependent catalysis by all the above DNA-based motors, competing models - for instance, that an increased rate of slippage slows the enzymes against high load without affecting the catalysis rate - remain formally possible. Myosin V, in contrast to these motors, has a step size large enough and a stepping rate slow enough to allow direct observation of dwell periods between steps under all relevant load and ATP conditions. My co-workers and I observed myosin V stepping against an elastic load (Mehta et al., 1999a). We measured the load corresponding to every observed dwell period separating two successive steps and preceding a forward step in the dual-bead trapping geometry, and we made two observations. First, the stepping rate at limiting (1 μM) ATP concentrations does not vary with load (Fig. 4, open circles). Second, the stepping rate at saturating (2 mM) ATP concentrations is independent

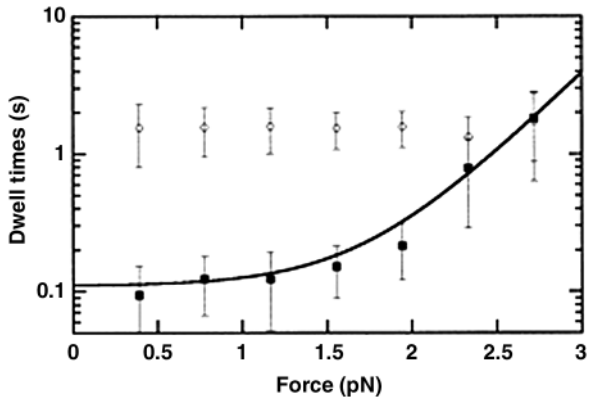

Fig. 4. Load-dependent dwell times separating adjacent step transitions and preceding forward-directed steps. Open boxes represent 1 μM ATP, and closed circles 2 mM ATP. The line traversing the closed circles reflects a fit of Eqn 3 to the data. Figure reproduced, with permission, from *Nature* (Mehta et al., 1999a).

of load below 1.5 pN and drops exponentially with loads above 2 pN (Fig. 4, closed squares).

The rate of stepping against ≤1 pN load (Eqn 2) exhibits Michaelis-Menten dependence on the ATP concentration (Rief et al., 2000).

$$\tau^{-1} = \varepsilon(F,[ATP])\,\frac{k_{cat}(F)[ATP]}{K_M^T(F) + [ATP]}$$

$$\tau^{-1} \sim \varepsilon(F,[ATP])k_{cat}(F) \quad \text{if} \quad [ATP] >> K_M^T$$

$$\tau^{-1} \sim \varepsilon(F,[ATP])[ATP]\,\frac{k_{cat}(F)}{K_M^T(F)} \quad \text{if} \quad [ATP] << K_M^T \qquad (2)$$

where F represents the load, ε the coupling ratio between chemical and mechanical cycling, K_M^T the ATP concentration required for cycling at half the maximal rate, and k_{cat} the cycling rate under saturating ATP concentration.

ε, k_{cat} and K_M^T are posed as functions of the external load, F, k_{cat} and K_M^T are functions of the various cycle rate constants. ε might depend on the ATP concentration, since potential kinetic partitioning into an unproductive catalytic cycle can depend on the transition rates of the productive one. K_M^T under a 1 pN force clamp (Rief et al., 2000) and in an unloaded gliding filament assay (M. Rief, unpublished) have both been measured at ~12 μM (Rief et al., 2000). ε has been measured at ~1 against 1 pN under all ATP concentrations (Rief et al., 2000). Below, I assume Michaelis-Menten dependence of the stepping rate against all loads.

Tight coupling between chemical and mechanical cycling means that ε=1, whereas loose coupling implies higher or lower values. Note that by 'coupling' I mean the link between a chemical cycle and a mechanical step in either the forward or backward direction. Hence, ε<1 implies cycling without movement. Investigators in the kinesin field have followed a different convention, one that considers the only meaningful coupling to be with mechanical steps in the forward direction (Svoboda and Block, 1994; Meyhofer and Howard, 1995; Coppin et al., 1997; Schnitzer and Block, 1997; Hua et al., 1997; Visscher et al., 1999). Owing to the distance and timescales of molecular stepping relative to thermal noise, kinesin does not allow direct identification of step intervals under low load and saturating ATP concentration. This makes a retreat and subsequent advance to restore the initial position indistinguishable from a period of mechanical quiescence. Hence, a significant presence of backward steps linked to chemical cycles would necessarily imply 'loose coupling', more than one chemical cycle per forward step. Since myosin V allows direct observation of step transitions under all load and ATP conditions, it demands a more nuanced vocabulary, one that distinguishes mechanical inactivity from successive backward and forward steps. Hence, discussion of myosin V focuses on dwell times separating two mechanical steps and preceding a forward-directed step. By contrast, most discussion of kinesin focuses on the velocity at which individual motors move (Svoboda and Block, 1994; Meyhofer and Howard, 1995; Coppin et al., 1997; Visscher et al., 1999). These differences in the observed variable and in the semantic convention must be kept in mind when one compares published observations in the two fields.

Since dwell periods at 1 μM ATP ([ATP]<<K_M^T) appear to be independent of load (Mehta et al., 1999a), ε(F, 1 μM) $k_{cat}(F)/K_M^T(F)$ is independent of the load F. Furthermore, if one neglects contrived scenarios in which load accelerates $k_{cat}(F)/K_M^T(F)$ and depresses ε(F, 1 μM) by the same fractional amount, ε(F, 1 μM) remains constant (~1) under all loads that the molecule can move against. Hence, the effective ATP-binding rate $k_{cat}(F)/K_M^T(F)$, encompassing binding of ATP and committing it to hydrolysis, does not vary with load. Note that kinesin, in which the binding of ATP is coupled to a significant conformational change (Rice et al., 1999), exhibits a load-dependent $k_{cat}(F)/K_M^T(F)$ (Visscher et al., 1999), which can be explained by a rapid and reversible load-dependent isomerization after reversible binding of ATP and necessarily before commitment to its hydrolysis (Schnitzer et al., 2000). Such models can be excluded for myosin V.

Load-dependent myosin V dwell periods at 2 mM ATP ([ATP]>>K_M^T) demonstrate that ε(F, 2 mM) $k_{cat}(F)$ remains independent of load below 1.5 pN and falls sharply as the load rises over 2 pN. One or both of the following scenarios might therefore be the case. (1) The coupling efficiency at 2 mM ATP falls sharply at >2 pN loads, even as the efficiency at 1 μM ATP remains independent of load. This suggests that branching to an unproductive cycle occurs more frequently from the state preceding ADP release than it does from the state preceding binding of ATP or its commitment to hydrolysis. (2) $k_{cat}(F)$ falls sharply at >2 pN loads. As per the above arguments, this requires $K_M^T(F)$ also to fall sharply at loads >2 pN. In the simplest model of one strain-sensitive biochemical transition per cycle, this transition can effect identical load dependence of both $k_{cat}(F)$ and $K_M^T(F)$. Such load-dependent chemistry offers a more efficient way than loss of coupling to fulfill the suspected organelle-tethering function of myosin V (Wu et al., 1998; Rogers and Gelfand, 1998; Mermall et al., 1998), for the same reason the Fenn effect enables a more efficient muscle response to arresting load. If attachments serve merely to bear tension without working against it, then it serves the molecule well to delay its dissociation from actin and thus better conserve ATP.

Additionally, if $k_{cat}(F)$ alone accounts for the observed load-

dependent dwell times, one can model the dwell times $\tau=k_{cat}(F)^{-1}$ using Boltzmann's law (Eqn 3):

$$\tau = \tau_1 + \tau_2 e^{Fd/kT} \quad (3)$$

where τ_1 represents load-independent transitions, τ_2 the load-dependent transition, F the load, d the characteristic distance over which load affects the catalysis rate, and kT the thermal energy (Wang et al., 1998).

Fitting this model to the data (Mehta et al., 1999a) shows that as the load F approaches zero, the load-dependent transition occurs a hundred times faster than the load-independent transitions. The load-dependent transition becomes rate-limiting at >2 pN. Load would affect the relevant transition rate over a characteristic distance - reflecting slippage, strain or arrested movement - of 10-15 nm, on the order of but less than the measured step size.

The observation that dwell periods do not vary with loads <1.5 pN indicates $\varepsilon(F, 2\ mM)\ k_{cat}(F)$ remains independent of loads <1.5 pN (Mehta et al., 1999a). Also, $\varepsilon(F, 2\ mM) \sim 1$ under 1 pN of load (Rief et al., 2000). If one dismisses ad hoc notions of exactly offsetting load dependences in $\varepsilon(F, 2\ mM)$ and $k_{cat}(F)$, the data show that $k_{cat}(F)$ remains independent of load below 1.5 pN. Hence, the rate-limiting transition, presumably ADP release, cannot depend on load. Some investigators have alluded to a load-dependent ADP release (Walker et al., 2000), but the apparent discrepancy could be semantic. Although the observed 12.5 s^{-1} transition rate does not vary with load, the rate of a transition from a slow-releasing ADP state to a 12.5 s^{-1} ADP-release state could very well depend on load. Such a transition has been proposed on thermodynamic grounds (De La Cruz et al., 1999) and is reminiscent of suggested transitions in other myosins (Jontes et al., 1997; Cremo and Geeves, 1998; Rosenfeld et al., 2000; Geeves et al., 2000).

As observed for kinesin (Svoboda and Block, 1994; Meyhofer and Howard, 1995; Coppin et al., 1997; Kojima et al., 1997), myosin V experiences reverse-directed steps. Unlike kinesin, in which the frequency of backward steps appears to be independent of load (Coppin et al., 1997; Visscher et al., 1999), myosin V experiences more reverse-directed steps under higher loads (Mehta et al., 1999a; Rief et al., 2000). At 1 μM ATP, dwell periods preceding forward steps (mean 1.62±0.15 sec, *n*=125; Mehta et al., 1999a) did not differ in mean from those preceding reverse steps (mean 1.44±0.18, *n*=62; Mehta et al., 1999a), which demonstrates that transition rates involved in backward steps are slower than those involved in forward steps. Note the relevance of semantic convention here: this is described as 'tight coupling' between ATP binding events and mechanical steps, the direction of the steps being a separate issue. The prevailing convention in kinesin study would cast this as 'loose coupling' ($\varepsilon<1$) between ATP binding events and forward steps.

Unlike kinesin, myosin V occasionally steps backwards two or three times in sequence (Mehta et al., 1999a). This implies that a 'ratcheting' and load-dependent strong binding transition to preserve the last forward step - like that suggested for kinesin (Coppin et al., 1997) - need not be considered for myosin V; the molecule concludes a backward step in a state competent to step backwards again. Additionally, when loads are rapidly oscillated between vanishing and super-stall levels, the fraction of steps occurring in the reverse direction are 13% (*n*=456) and 37% (*n*=107) at 2 mM and 1 μM ATP respectively (computed from Table 1 of Mehta et al., 1999a). This suggests that kinetic partitioning into a reverse-step process occurs from states that precede ATP binding or its commitment to hydrolysis.

The step size

Because adjacent monomers in an actin filament are arranged helically and not linearly, a processive motor moving from one monomer to the next would spiral around the track and consequently make vesicle transport problematic. A myosin motor could, however, step across the long-pitch pseudo-repeat of the actin helix, reaching from one actin monomer to the next one sharing the same azimuth, and thus linearize its track. This is no small feat, since the required step distance would span 13 actin subunits and 36 nm, larger than any other molecular step distance observed to date. Some observers had long speculated that the unusually long, 23-nm neck region (Cheney et al., 1993) evolved so the two heads could bind an actin filament while separated by the 36 nm pseudo-repeat distance (Howard, 1997). Moreover, this neck region resembles a molecular lever for myosin II, amplifying a small conformational change within the motor domain (Uyeda et al., 1996; Anson et al., 1996; Suzuki et al., 1998; Dominguez et al., 1998; Corrie et al., 1999; Warshaw et al., 2000; Shih et al., 2000; Ruff et al., 2001; but also see Tanaka et al., 2000; Molloy et al., 2000). Myosin V may require its long neck to leverage motor domain shape changes into 36 nm steps.

Initial observation of chick myosin V stepping employed the dual-beam geometry of Finer et al. (Finer et al., 1994). Myosin V pulled suspended individual actin filaments in discrete steps of 15-40 nm. These distances reflect movement not of the molecule but, rather, of a bead in a stationary optical trap and attached to a single actin filament. Potentially non-linear elastic linkages separating the bead from the filament, or separating the molecule from the microscope coverslip surface, could absorb some of the molecular step distance, masking it from our view.

To circumvent the series elasticity problem, we moved one optical trap through large-amplitude triangle-wave oscillations while isolated myosin V molecules bound and moved the attached actin filament (Mehta et al., 1999a). In the absence of myosin binding, the beads followed the waveform of the optical trap. Upon myosin binding, however, one of the beads exhibited clipping of this waveform in areas of maximum tension. Such clipping indicates that, during the high-tension phase of each trap oscillation cycle, the trap continues to move but the bead no longer follows it; this effect requires - and hence demonstrates - that all connections separating the bead from the surface are rigid relative to the optical trap. Hence, stepwise advances of the clipped level accurately reflect protein movements. Multiple data sets at various ATP concentrations and trap oscillation frequencies produced data distributions centered around 34-38 nm, demonstrating that the molecule indeed has the large step size required to linearize its helical track. Both forward and backward steps were of this size. The distribution widths remained large, with standard deviations of individual data sets ranging from 5 nm to 11 nm. This suggested that the myosin V molecule does not step along the pitch pseudo-repeat precisely but does so only on average; this is probably still sufficient to avoid problematic spiraling

behavior. However, these experiments left open the possibility that limited rotation of the trapped filament, over the 0.1-1 sec dwell periods separating step transitions, could generate a random shift in the next available actin monomer bearing the necessary azimuth, hence spreading the step measurement distribution. Since an optically trapped 1 μm bead exhibits a rotational persistence time of ~1 second (Einstein, 1956), significant rotation of the trapped beads can occur between successive molecular steps. Veigel et al. measured similar step distributions of murine myosin V, also using the dual beam geometry (Veigel et al., 2001). Rather than oscillating one of the traps, they characterized the series elastic element and corrected the raw data for its effects.

Rief et al. observed chick myosin V stepping in a force-clamped single-bead assay, which allows observation of longer step sequences and meaningful analysis of stepping kinetics (Rief et al., 2000; see above). An additional advantage is that any elastic connections remain similarly strained throughout the range of stepping and thus cannot absorb any displacements produced by the attached motor (Visscher and Block, 1998). Furthermore, the actin filament is mounted upon a surface and cannot rotate. We observed regular steps of mean 40.2 nm, matching earlier measurements within calibration uncertainties, which were unusually high owing to the small size of the beads used. The distribution standard deviation of several data sets combined narrowed to a still uncomfortably large 6.4 nm. Moreover, the motor exhibited occasional 20-nm step advances under 2 pN load conditions. The dwell periods following 20 nm steps, which lasted seconds and always ended with an added 20 nm advance or retreat, exhibited high bead-position variance and thus a less rigid linkage with the surface. The relative rarity of such steps suggests that they involve transitions off the normal cycling pathway, and it remains difficult to interpret them. Nevertheless, the motor might have advanced part of its unitary step distance, adopted a less rigid linkage with the track involving only one bound head, and could then have retreated or advanced the remainder of the unitary step after a pause.

Step size measurements are consistent with electron microscopic observation of apparently walking myosin V molecules. Walker et al. imaged actin filaments decorated sparsely with baculovirus-expressed murine-sequence myosin V dimer fragments (Walker et al., 2000). Under some conditions, they observed a fraction of dimers with both heads bound to the same double helical actin filament separated by 9-17 actin subunits (Fig. 5). The dominant peak in the distribution reflected head separation by 13 actin subunits, one 36-nm pseudo-repeat, but subsidiary peaks appeared at 11 and 15 subunits, in agreement with the spread in observed step lengths. Hence, structural observations further supported the notion that myosin V steps across the actin pseudo-repeat only on average and not precisely and sometimes misses the 13th subsequent subunit by two or four subunits in either direction. Such variability in the step measurement could either derive from an erratic molecular walk or from conformational disorder within the actin filament (Egelman and DeRosier, 1992).

Walker et al. observed such putative walking intermediates in the presence of ADP or subsaturating (1-100 μM) ATP concentrations (Walker et al., 2000). They did not observe clear structures in the absence of nucleotide. To bind a single filament with two heads 36 nm apart, the motor domains require a strong asymmetry in their preferred orientation - one leads and the other trails. The authors concluded that nucleotide-free conditions do not produce this necessary asymmetry, since both heads presumably prefer the post-stroke (trailing head) intermediate (Dias et al., 1997). They further concluded that ADP alone can produce the required asymmetry and therefore that the presumably pre-stroke leading head in the walking intermediate might be ADP bound. Alternatively, both heads could adopt distinct ADP-bound states. Observations at low ATP concentration suggested that the intermediate preceding ATP binding also has both heads bound, presumably because the trailing head remains nucleotide free while the leading head has a bound ADP. Hence, the molecule awaits ATP binding to switch its trailing head into a low-affinity state. The authors also observed asymmetric strain in the walking intermediate, the neck nearest the barbed filament end, to which the molecule usually travels (Cheney et al., 1993; Wolenski et al., 1995); it was arced as if attempting to pull the lagging head forward. Such strain could allow asymmetric and/or coordinated chemistry between the two motor domains.

The leading head in such walking intermediates is presumably trapped in a pre-stroke intermediate, of the sort that is so transiently populated in myosin II as to defy experimental access to date (but see Uyeda et al., 2001). Hence, the micrographs of walking intermediates may provide the first high-resolution images of an actin-bound myosin in its pre-stroke state, a textbook example of Pollard's (Pollard, 2000) 'switch and win' strategy - when a target protein denies experimental access to something, abandon it for a more accommodating relative. Intriguingly, the head-neck angle adopted by the leading head in the observed walking intermediate resembles that adopted by isolated (actin-free) myosin V molecules in solution with ATP (Burgess et al., 2001); these molecules are presumably trapped in an ADP-Pi state. The head-neck orientation adopted by the trailing head resembled that of isolated myosin V molecules in the absence of ATP (Burgess et al., 2001).

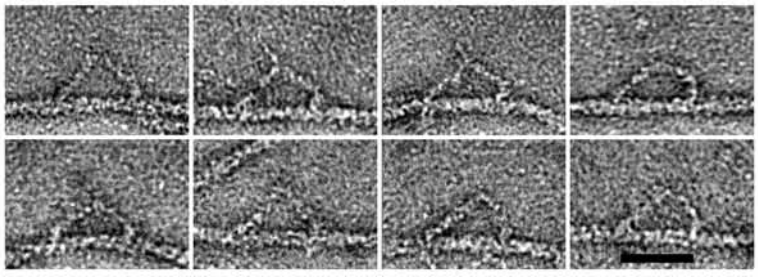

Fig. 5. Electron micrographs of single myosin V molecules attached to single actin filaments. The shown molecules have two motor domains spaced by 13 subunits, which is the most common spacing observed. Several molecules appear to mimic a snowboarder's riding stance, in which their leading neck arcs forward, as if under tension to move forward. Figure reproduced, with permission, from *Nature* (Walker et al., 2000).

Curiously, Walker et al. observed only single head attachments, and many heads dissociated at 1 mM ATP and in 100 mM KCl (Walker et al., 2000). However, this finding may have origins in the method of specimen preparation (P. Knight, personal communication). Moreover, these experiments involve expressed HMM constructs that have not yet been observed to behave processively (Moore et al., 2001). It remains possible that such constructs are weakly processive and thus detach frequently from the track under saturating ATP conditions (Walker et al., 2000). Alternatively, the kinetically dominant intermediate under saturating ATP may have only one head strongly bound to actin.

The product of a ~36-nm step (Mehta et al., 1999a; Rief et al., 2000; Walker et al., 2000; Veigel et al., 2001) and a ~3-pN stall force (Mehta et al., 1999a) exceeds 100 zJ, the energy released by a single ATP hydrolysis under physiological conditions (Bagshaw, 1982). Observations of tight chemomechanical coupling between ATP hydrolysis and mechanical steps, even against high loads (see above), might lead to predictions of unusually high efficiency in converting chemical energy to mechanical work. Such predictions neglect the incidence of ATP-consuming reverse steps against high loads. If an ensemble of molecules were pre-loaded at ~2-3 pN, a large fraction would proceed to step backwards and perform negative work, making the ensemble efficiency, the only meaningful thermodynamic variable, far less than 100%. Nonetheless, the observed frequency of apparent 'super-energetic' steps (work output exceeds mean free energy input) should be rather small on statistical mechanical grounds (see Landau and Lifschitz, 1980). Three factors could explain such observations. First, the motors do not move against 3 pN; the most energetic observed forward steps, against somewhat smaller loads, should fall short of producing 100 zJ and hence occur frequently. Second, the above described ~36 nm step measurements - in which elastic linkages have been finessed out of the experiment - do not involve loads in excess of 2 pN. The molecule may thus advance by <36 nm when facing higher loads. Third, the free energy released by ATP hydrolysis under experimental flow cell conditions in the presence of an ATP-regenerating system may be slightly higher than 100 zJ.

Although various experiments demonstrate that myosin V walks with a stride length of 36 nm, the potential for smaller substeps within this stride remains unclear. Walker et al. observed the head-neck junctions in walking intermediates in averaged electron micrographs (Walker et al., 2000). On the basis of the difference between the head-neck angle describing the leading head and that describing the lagging head, they estimated that a shape change in the motor domain could account only for a 26 nm advance. Moreover, Veigel et al., using a dual-beam optical-trapping geometry, measured 20-25-nm unitary steps (non-processive) produced by a truncated monomer fragment containing one motor domain and six IQ repeats bound to light chains (Veigel et al., 2001).

On the basis of these data, Walker et al. (Walker et al., 2000) have suggested that a ~20-26 nm conformational change must be supplemented by ~10-16 nm - an estimate that, intriguingly, accords well with the characteristic distance associated with load-dependent mechanochemistry (above). This supplement may reflect a diffusive search that strains the molecule (Walker et al., 2000; see also Huxley, 1957). However, there are three reasons to question this hypothesis. Firstly, this required diffusion to induce strain would probably span on the order of a millisecond in the absence of external load (see Berg and von Hippel, 1985). Load should slow this search significantly: the 2 pN clamp (Rief et al., 2000) imposes upon the molecule 1.8 to 2.2 pN of tension; the *minimum* energy barrier confronting the hypothetical diffusion is thus 10-16 nm×1.8 p*N*=18-29 zJ=4.5-7.2 kT. By Boltzmann statistics (see Landau and Lifschitz, 1980), such loading will slow the search by at least $e^{4.5-7.2}$~100-1000-fold, meaning the search will take ~0.1-1 second on average. Under this 2 pN clamp, however, we observed rapid ~36-nm steps with <3-ms rise times and no apparent intermediate dwell (Rief et al., 2000). Altough we observed occasional 20 nm substeps, followed by dwells spanning seconds (above), the relative rarity of these smaller steps suggests that the associated transitions are off the normal kinetic pathway. Secondly, the notion of a biased diffusive search that strains the molecule might predict that the stride length would more often fall short of 36 nm than exceed it, especially in solution studies where isolated molecules need not follow linear trajectories along the helical actin track. By contrast, electron micrographs of walking intermediates (Walker et al., 2000) show the opposite asymmetry: the molecule more often steps to the 15th following subunit than it does to the 11th. Thirdly, the angle change measured in the averaged electron micrographs may underestimate the actual shape change in the motor domain, especially if the leading head in these images has already executed a partial power-stroke then arrested by internal load. Although the measured 20-25 nm monomer step size (Veigel et al., 2001) dovetails nicely with the structure-based estimate (Walker et al., 2000), there is no evidence that this measurement matches the power stroke of an intact dimer in stride.

Molecular models for processive myosin V motion

It might seem premature to posit models for myosin V processivity, given our lack of solution kinetic data from the intact dimer. Nonetheless, several such models have been proposed. On the basis of the above data, I believe any model should accommodate the following observations.

(1) Myosin V is a highly efficient processive motor (Mehta et al., 1999a; Sakamoto et al., 2000; Rief et al., 2000) that moves in steps averaging 36 nm (Mehta et al., 1999a; Rief et al., 2000; Veigel et al., 2001).

(2) The molecule couples ATP binding events tightly to mechanical steps. This remains true under all observed loads at limiting ATP concentrations and at least for loads below ~1.5 pN at saturating ATP concentrations (Rief et al., 2000).

(3) A 12-18 s^{-1} ADP release is rate-limiting during steady-state cycling of expressed monomers (De La Cruz et al., 1999; De La Cruz et al., 2000b) and tissue-purified dimers (Rief et al., 2000).

(4) This rate-limiting transition is independent of load (Mehta et al., 1999a; Rief et al., 2000).

(5) When ADP rebinding slows the cycling rate, the release of post-hydrolysis ADP and the release of rebound ADP occur at similar rates (De La Cruz et al., 1999; Rief et al., 2000).

(6) ATP binding promotes rapid dissociation of monomer fragments from actin (Trybus et al., 1999; De La Cruz et al., 1999; Wang et al., 2000; De La Cruz et al., 2000a).

(7) The dissociated myosin head hydrolyzes ATP quickly

(Trybus et al., 1999; De La Cruz et al., 1999; De La Cruz et al., 2000a)

(8) Myosin-ADP-P_i monomers bind actin and then release P_i quickly (De La Cruz et al., 1999; De La Cruz et al., 2000a).

(9) Myosin and myosin-ADP bind actin with high affinity (Trybus et al., 1999; De La Cruz et al., 1999).

(10) The rate of ATP binding and its commitment to hydrolysis (k_{cat}/K_M^T) is independent of load (Mehta et al., 1999a).

(11) A load-dependent transition might become rate-limiting at saturating ATP concentrations, but only at loads exceeding 2 pN. Under vanishing load, this transition occurs >100 times faster than the rate-limiting step (Mehta et al., 1999a; >1200 s^{-1}). These conclusions assume that tight chemomechanical coupling is preserved at high load.

(12) A kinetically prevalent intermediate state, at least at limiting ATP concentrations, has both heads bound to actin, 36 nm apart on average (Walker et al., 2000).

(13) Intramolecular strain affects the two bound heads asymmetrically (Walker et al., 2000).

(14) Reverse-directed stepping occurs under high load and more often at limiting ATP concentrations than at saturating ATP concentrations (Mehta et al., 1999a).

(15) The kinetics of reverse stepping do not differ from the kinetics of ATP binding and forward stepping at limiting ATP concentrations (1 μM ATP, 1 s^{-1} rate of stepping and of ATP binding, see above).

Our preferred model (Rief et al., 2000; see also Vale and Milligan, 2000) presents the most straightforward scheme to account for available kinetic data (Fig. 6). Initially, both heads are strongly bound to actin; the leading (pre-stroke) head is ADP bound, and the rear (post-stroke) head is nucleotide-free (12). ATP binds the trailing head, promoting its rapid dissociation (6). Intramolecular strain is then discharged in a power stroke that moves the detached head forward to become the new leading head, a process that may or may not involve a succession of smaller substeps. The new leader rapidly hydrolyzes ATP (7) and binds actin (8). The events between dissociation and rebinding - in effect commitment to hydrolysis of ATP - cannot be rate limited by a slow rebinding immediately following a fast and reversible conformational change (Schnitzer et al., 2000) or by a slow conformational change. If it were, the commitment to ATP hydrolysis would be rate limited by a necessarily load-dependent movement, and the scheme would violate (10). Once the new leader rebinds actin, it rapidly releases P_i (8) and strains the trailing head towards forward movement (13). The trailing head remains bound to its actin site and to ADP. The following transition, a rate-limiting (3,5) and load-independent (4) ADP release from the trailing head, completes the cycle. Hence, the kinetically dominant intermediate at saturating ATP concentrations has both heads bound strongly to actin, a prediction that has not yet been verified.

Before the trailing head releases its ADP, the leading head must retard its ADP-release rate to prevent a futile turnover event. This can be accomplished by intramolecular strain (13): the asymmetry in the direction of strain experienced by the two heads can maintain the leading head, which is strained against its direction of movement, in a slow ADP-release state. In the absence of such strain, the motor domain rapidly moves out of this state, thus preventing kineticists from observing a second, slow ADP-release rate in monomer solution studies. Similar strain could account for (11), in which the transition from this slow ADP-release state to the ~12 s^{-1} ADP-release state - now in the *trailing* head - becomes rate limiting under high externally applied load against the direction of movement (this transition would reflect τ_2 in Eqn 3 above).

In this model, processivity hinges on a race: once the trailing head dissociates, the leading (bound) head undergoes an isomerization from a slow ADP-release state to a ~12 s^{-1} ADP release state, releases ADP, binds ATP and then dissociates from actin. This sequence of events must be outpaced by the free head moving forward and rebinding actin, or the molecule will jettison its track; the degree of processivity will depend on the relative rates of bound head dissociation and free head rebinding. This model predicts greater processivity under limiting ATP. Such a kinetic competition differs from the hand-over-hand model presently reigning over kinesin, in which binding of the leading head induces release of the rear one (Hackney, 1994; Gilbert et al., 1995; Ma and Taylor, 1997; Gilbert et al., 1998; Hancock and Howard, 1999; Crevel et al., 1999). Whereas hand-over-hand movement has been intimated for myosin V (De La Cruz et al., 1999), it is difficult to reconcile with observations that stepping dimers and solution

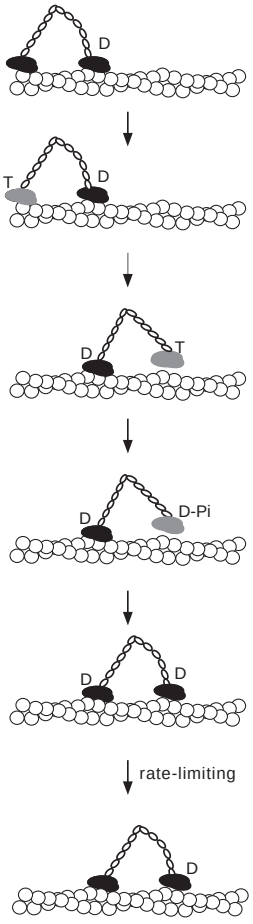

Fig. 6. Molecular model proposed by Rief et al. (Rief et al., 2000). Grey motor domains correspond to weak (low affinity) binding to actin, and black motor domains correspond to strong (high affinity) binding to actin.

monomers cycle at the same, ~12 s^{-1} rate. By contrast, during ATP turnover, monomeric kinesin releases microtubules more slowly than dimers cycle (Hancock and Howard, 1999), which suggests that each head of the intact dimer accelerates microtubule release by its partner.

An alternative model of myosin V processivity (E. M. De La Cruz, personal communication) proposes that the kinetically dominant steady-state intermediate in the presence of saturating ATP has the trailing head strongly bound (K_d<1 μM) and the leading head weakly bound (K_d>1 μM) to actin (12). The trailing head has bound ADP, and the leading head is in an ADP-P_i state. ADP release from the trailing head is rate limiting (3,5) and load independent (4). Two cues synchronize the cycles of the sister heads. First, resistance from the trailing head inhibits strong binding by the leading head and thus slows an otherwise-fast (8) P_i release. Second, ATP binding to the rear-head, dissociates it from actin (6) and relieves this inhibition. The leading head then binds actin strongly, undergoes its power stroke and *then* releases P_i rapidly; the power stroke requires a force-exerting ADP-P_i state (see Dantzig et al., 1992). If the trailing head dissociates from actin with the leading ADP-Pi head off actin, the motor jettisons its track. Alternately, if the trailing head dissociates when the leading head is bound to actin, the motor steps forward. This kinetic competition remains independent of ATP binding, and thus the degree of processivity remains independent of ATP concentration. However, the kinetically dominant nucelotide states of the heads depend on the ATP concentration, as elaborated below.

Both models readily accommodate repeated backward steps. In our model, a forward step requires that a trailing head release ADP, bind ATP and release actin. If these events are outpaced by a leading head isomerizing slowly to a ~12 s^{-1} ADP-release state, releasing ADP and binding ATP, then the leading head will release actin, hydrolyze ATP, and either rebind actin at the same site (futile hydrolysis) or move backwards under load and then rebind (reverse step). Upon rebinding actin, the formerly leading head releases Pi. Owing to the slow isomerization, the forward step enjoys a dominant kinetic advantage over the futile/reverse one, but this advantage grows less imposing as ATP becomes scarce, which is consistent with (14). Both forward and reverse steps will occur at the ATP binding rate (15) provided that the reverse-step pathway remains slow relative to ATP binding (i.e. that the reverse step pathway remains rate limited by the slow isomerization in the leading head). Such a reverse step concludes either with both heads ADP bound (on pathway) or with the new leading head nucleotide free and the new trailing head ADP bound (off pathway). If the latter, the molecule will either experience an ATP binding and futile hydrolysis at its leading head or an ATP binding following ADP release at its trailing head. Either transition returns the molecule to an on-pathway intermediate.

In the De La Cruz model, the leading head remains trapped in an ADP-Pi state that frequently releases actin. Under load, it can release actin and slip backwards while its sister head remains strongly bound to actin either with ADP or nucleotide free (9). The result is an off-pathway intermediate in which the new leading head (following the reverse step) is strongly bound while the new trailing head binds actin and releases its Pi from a post-stroke position. The new leading head releases its ADP (if bound), binds ATP, dissociates from actin (6) and hydrolyzes the ATP (7). Under saturating ATP, this sequence of events occurs at ~12 s^{-1} (if the new leading head had ADP tightly bound at the onset of the reverse step) or faster (if it had not). In parallel, the new trailing head proceeds to release its ADP at ~12 s^{-1}. If the leading head reaches its ADP-Pi state before the trailing head binds ATP, the molecule returns to its normal kinetic pathway. If it doesn't, the leading head is presumably unable to execute a power stroke and a futile turnover occurs, as the trailing head, dissociating actin and hydrolyzing ATP, rebinds actin and jettisons Pi without a unitary advance. Since a reverse step can occur anytime the leading head dissociates and the trailing head remains strongly bound, the relative incidence of reverse steps should be greater under limiting ATP conditions (14). When the ATP concentration falls, a slow and ATP-independent slippage of the leading head can better compete kinetically with ATP binding to the trailing head. Provided that this slippage rate remains slow relative to ATP binding, forward and backward steps both occur at the rate of ATP binding (15).

Under extreme ATP starvation, both of these models predict deviations from Michaelis-Menton dependence of motor speed on the ATP concentration: the motors move more slowly. In our model, both heads will eventually reach (different) equilibria binding with solution ADP, and both heads can be nucleotide free. Hence, ATP can sometimes bind the leading head instead of the rear one. Since a power stroke reflects discharge of intramolecular strain when the trailing head binds ATP, forward steps remain frequent. In the De La Cruz model, leading head P_i release may outpace trailing head ATP binding. Since a successful power stroke requires the trailing head to bind ATP and dissociate from actin, the molecule rarely steps forward in the same manner. Rather, there are two possible outcomes: (A) the leading head experiences frequent unproductive cycles, turning over ATP in the process and perhaps slipping backwards under load; or (B) the leading head attempts to undergo its power stroke and strains the molecule (13), perhaps in this regime 'switching' to our model - the strain would be discharged into a power stroke once the rear head dissociates. Regarding both models, 'extreme ATP starvation' means an ATP binding rate that is slow relative to hypothetical transitions - either ADP or Pi release from the leading head - perhaps slower than 1 s^{-1}. Experiments to date have not explored ATP concentrations below 1 μM (1 s^{-1} ATP binding), and so these scenarios may remain untested.

A third, reported model (Walker et al., 2000) has since been revised in light of new data (P. Knight, pers. commun.). Another class of models has been proposed and involves loose coupling between cyclical conformational changes and ATP hydrolysis events in myosin V (Yanagida et al., 2000a). A succession of smaller conformational changes culminate in a net advance of 36 nm per ATP hydrolyzed (Yanagida and Iwane, 2000b), which is similar to models of myosin II proposed by Yanagida and colleagues (Yanagida et al., 1985; Kitamura et al., 1999). Such a model for myosin V sits uneasily alongside (8), (9) and (12). Nevertheless, a recent experiment (Tanaka et al., 2001) suggests that a myosin V dimer construct that has a severely shortened neck region containing only one IQ repeat rather than the native six is capable of moving an actin filament through a succession of 3-5 36-nm advances! This rather iconoclastic result seems consistent with an

incremental molecular inchworming along the actin rather than a unitary advance in which one head swings forward to reach ~13 actin subunits in front of the other; the short neck cannot accommodate so large a swing. However, these data remain preliminary.

An alternative version of the loose coupling model involves a succession of 36-nm steps resulting from a single ATP hydrolysis. Although this sits more comfortably with (12), it renders (8) and (9) awkward. Moreover, it conflicts directly with (2). Yanagida and Iwane (Yanagida and Iwane, 2000b) attempt to counter this by emphasizing an argument by Sakamoto et al. (Sakamoto et al., 2000). Although the processive dimer moves at speeds of up to 1 μm/s in their assay, solution ATPase measurement of the intact dimer, even using the NADH-coupled assay to prevent ADP accumulation (T. Ando, pers. commun.), yields only 2.4 s^{-1}. Dividing the two numbers suggests a movement of 400 nm per ATPase cycle.

The primary problem with this and all such comparisons is that the ATPase measurement reflects the average properties of proteins in solution, whereas the motility measurements could reflect a minority of proteins able to move. Sakamoto et al. make precisely this point in qualifying their numbers (Sakamoto et al., 2000), and it seems especially relevant here, since many ATPase measurements of the tissue-purified dimer show unusually low and potentially inhibited, Ca^{2+}-sensitive rates (Cheney et al., 1993; Nascimento et al., 1996). In order to determine a unitary step corresponding to observed motile proteins, one must make a different measurement of the same motile proteins. For instance, a fluctuation analysis (Svoboda et al., 1994; Schnitzer and Block, 1997) of moving fluorescent molecules on single actin filaments at limiting ATP concentrations, analogous to the stepping rate measurements of Rief et al. (Rief et al., 2000), should allow an estimate of the displacement per ATP hydrolyzed by active molecules. In light of the above data, I expect this measurement to yield approximately 36 nm.

Conclusions and future directions

A broad variety of experiments have thus demonstrated that myosin V is a highly efficient processive motor whose cycle rate is limited by ADP release and whose average step distance approximates the actin long-pitch pseudo-repeat. These studies dispel the notion that processivity is a hallmark of microtubule- and not actin-based motors. They also suggest an explanation for why many nonprocessive myosins exist as dimers even though the two heads appear in most assays to behave independently (Hackney and Clark, 1984; Harada et al., 1987; Tanaka et al., 1998; Ruff et al., 2001; for dissent see Conibear and Geeves, 1998; Tyska et al., 1999 and Ito et al., 1999): perhaps an ancestral protein needed two heads to walk.

Although kinesin and myosin V are both processive motors and thus merit extensive comparisons, note that kinesin operates as if in a ‘lower gear’ than myosin; it traverses a much smaller distance per ATP hydrolyzed but can generate considerably greater force. Mounting evidence that myosin V and kinesin interact directly (Rogers and Gelfand, 1998; Huang et al., 1999) gives this difference potential physiological relevance: 3 pN loads that would arrest one myosin V and perhaps force it to move backwards (Mehta et al., 1999a) will scantly even slow the rate of forward progress of one kinesin (Visscher et al., 1999). It remains possible that isolated processive motors allow cargo transport to shift seamlessly between microtubule and actin tracks; the kinesin might simply overpower the myosin V in case of competition. Although kinesin and myosin V exhibit significant differences under load, the resemblance in single molecule run lengths (Vale et al., 1996; Romberg et al., 1998; Sakamoto et al., 2000) and speeds (Howard et al., 1989; Cheney et al., 1993; Mehta et al., 1999a) is intriguing.

What does processivity mean for a cell seeking to maintain its traffic? Processivity could allow one or a few motors to transport cargo, but it is not necessary. A few high duty-ratio, non-processive motors support movement under in vitro conditions (Hancock and Howard, 1998) and can probably do so more readily within the cytoplasm, where macromolecular crowding effects (see Ellis, 2001) will restrict motor and cargo diffusion away from the actin track. Hence, the biological role of processive motors remains unclear. Are single molecules used for cargo transport? Precious little data address this question, as regards myosin V or even kinesin, whose study is a decade older. Although electron micrographs illustrate putative single kinesin attachments to vesicles (Hirokawa, 1982), such evidence remains sketchy. Myosin V study lacks even this level of detail. The experiments reviewed here demonstrate its abilities, and it must be left to other assays, some using sophistications of presently nascent experimental technology (see Byassee et al., 2000), to show that myosin V exploits these abilities in vivo.

Solution kinetic study of the myosin V dimer certainly ranks among the most important ongoing efforts to understand the molecule. To behave processively, the dimer must ensure that the relative behavior of the two heads allows sequential stepping and catalysis. A motor can achieve this by rendering the advance and rebinding of a detached head much faster than dissociation of a bound head, as suggested in the above models for myosin V. This proposal differs radically from the scheme presently favored for kinesin: a coordinated ‘hand-over-hand’ movement, in which the trailing head releases only after receiving a signal that the leading head has bound. A litany of solution kinetic measurements of kinesin dimers point to this model (Hackney, 1994; Gilbert et al., 1995; Ma and Taylor, 1997; Gilbert et al., 1998; Hancock and Howard, 1999; Crevel et al., 1999), although its particulars remain controversial (see Schief and Howard, 2001). However, the most accepted rendition of either scheme involves a leading head and a lagging head that swap roles with every unitary advance. Recent evidence has called this into question: any such swapping of roles requires a significant (probably ~180°) molecular rotation accompanying every unitary advance, and no such rotation of beads bound to single kinesin molecules has been observed (Hua et al., 2001; Chung et al., 2001). Myosin V awaits similarly detailed kinetic and biophysical analysis. Alternative models of processive movement by one head alone, analogous to those proposed for other motor proteins (Sakakibara et al., 1999; Okada and Hirokawa, 1999; Okada and Hirokawa, 2000), are at odds with the kinetic non-processivity of monomeric myosin V (Trybus et al., 1999); I do not believe they will prove relevant here.

One pressing experiment involves processive ATP hydrolysis by dimers in solution. Although kinesin comparisons may by now seem hackneyed, it merits mention

that direct and definitive measurement of highly processive ATP hydrolysis (Hackney, 1995) followed the initial demonstration of processive movement (Howard et al., 1989) by six years. Investigators were long vexed by tail-induced auto-inhibition of kinesin molecules in solution but not of those on surfaces (Hackney et al., 1992; Friedman and Vale, 1999; Coy et al., 1999b; Hackney and Stock, 2000), a phenomenon that may have analogs in myosin V. Several labs have measured very low or even zero ATPase activity by tissue-purified myosin V dimers in the presence of EGTA (Cheney et al., 1993; Nascimento et al., 1996; Sakamoto et al., 2000), a condition that supports processive motility of surface or bead-bound motors (Mehta et al., 1999a; Rief et al., 2000) and at least some motors in solution (Sakamoto et al., 2000). Although Ca^{2+} increases the actin-activated ATPase rate of the chick or murine tissue-purified dimer (Cheney et al., 1993; Nascimento et al., 1996; Wang et al., 2000), it also suppresses motility (Cheney et al., 1993; Nascimento et al., 1996) permanently unless exogenous CaM is added (but note discrepant reports regarding analogous effects on truncated constructs: Trybus et al., 1999; Homma et al., 2000). Only HMM constructs lacking the cargo-binding domain maintain apparently uninhibited ATPase rates in the presence of EGTA (Wang et al., 2000; Homma et al., 2000). However, such truncated dimers have not been observed to move processively (Moore et al., 2001). Moreover, they do not appear to be kinetically processive. Hackney's method relies on the actin-activated ATPase rate, V, under limiting actin concentration (Eqn 4):

$$V = \frac{k_{cat}}{K_M^A}\,[\text{Actin}] \qquad (4)$$

where K_M^A reflects the actin concentration required for half maximal activation. k_{cat}/K_M^A can be compared with the second-order bimolecular association rate k_a, the occurrence rate of actomyosin collisions that result in Pi release and hence at least one actin-activated ATP hydrolysis. A k_{cat}/K_M^A in excess of k_a provides a signature of multiple ATP hydrolysis cycles per diffusional encounter (Hackney, 1995). The best available estimate for the monomer fragment k_a derives from the actin-dependent Pi burst measurements made by De La Cruz et al., 4.6×10^6 M^{-1} s^{-1} at 25°C (De La Cruz et al., 1999). A k_a characterizing the intact dimer may differ from this but cannot exceed a diffusion-limited collision rate of the order of 10^7 M^{-1} s^{-1} at room temperature. The HMM dimer construct of Wang et al. exhibited a k_{cat}/K_M^A of 2.5×10^7, at 25°C and 80 mM KCl (Wang et al., 2000), indicating only ~2-5 ATPs hydrolyzed per diffusional encounter between the dimer fragment and actin - weak processivity at best. By a similar calculation using published data (Nascimento et al., 1996; Wang et al., 2000; both at 37°C), chick and murine tissue-purified dimers, in the presence of sufficient Ca^{2+} to activate their ATPase rate but inhibit in vitro motility, do not exhibit processive chemistry. Observation of processive ATP turnover by myosin V - preferably under conditions that support processive in vitro motility - may prove rather challenging.

Other questions include the following. (1) Will dimers equilibrated with ATP and then flushed with actin release one or two P_i in a fast burst upon binding actin? Thus far, evidence for two - walking intermediates observed with ADP alone (Walker et al., 2000) and fast Pi release upon actin binding by monomer fragments equilibrated with ATP (De La Cruz et al., 1999) - remains circumstantial. Observations that kinesin dimers release only one of two tightly held ADPs upon binding microtubules (Hackney, 1994) motivated the work that appeared to clarify the coordinated hydrolysis cycles of the two heads (Gilbert et al., 1995; Ma and Taylor, 1997; Gilbert et al., 1998; Hancock and Howard, 1999; but see also Hua et al., 2001; Chung et al., 2001). If myosin V dimers release only one of two tightly held P_i molecules upon binding actin, this implies that the leading head remains in a weakly bound ADP-Pi state while the lagging head remains strongly anchored with ADP, which would favor the De La Cruz model described above. What conditions will then promote or retard release of the second Pi? (2) Will the actin-bound dimer exhibit two different ADP binding rates and affinities? This property has been observed for kinesin (Ma and Taylor, 1997) and seems to be a requirement if the two heads are to coordinate their chemical cycles. (3) How vital is the 23-nm neck for processive movement? Will a dimer that has four, five or seven IQ repeats per neck perform like the native dimer that has six? Some of these may behave more or less processively than the native protein, and perhaps some will move processively but with different stride lengths and along a spiral trajectory. Moreover, if a thermally driven search for a binding site follows and supplements a conformational change (Walker et al., 2000), perhaps different neck length constructs would be more or less adept at and revealing of this diffusive search. (4) How has myosin V tuned its kinetic parameters to allow for processive chemistry? Several lines of evidence link flexible loops in the myosin II motor domain to affinities for actin and ATP (for review, see Murphy and Spudich, 2000). Does myosin V rely on its loop sequences for the kinetic adaptations that allow processive movement? Swapping loops between varied myosin classes should generate interesting chimeras that may or may not behave processively. (5) Does the run length or, equivalently, the degree of processivity depend on the ATP concentration? Above models reach very different conclusions in this regard. If the molecule follows a kinetic processivity scheme, such data will address the question of whether ATP binding is involved in the rate of bound head dissociation competing with the rate of free head binding. (6) Along similar lines, does the molecule undergo significant rotation with every unitary advance (see Chung et al., 2001; Hua et al., 2001)? What might this suggest regarding models in which the two heads swap roles with every unitary advance (see Fig. 7)? (7) Does the molecule preserve tight chemomechanical coupling against high axial loads at saturating ATP concentrations? If so, what is the strain-sensitive biochemical transition that becomes rate limiting under high load? (8) The above described load-dependence measurements concern loads applied to the actin, against the direction of myosin V movement. How will this movement be affected by lateral loads that either pull the motor away from its track, perpendicular to the specimen plane (see Gittes et al., 1996), or pull it perpendicular to its direction of motion in the specimen plane (see Lang et al., 2001)? Such results should address the geometry of the relevant conformational changes that might be rendered rate limiting by application of external loads. Moreover, will the motor accelerate under loads along

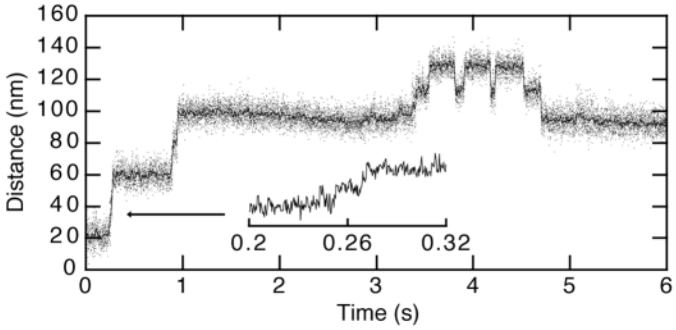

Fig. 7. Limping behavior, observed extremely rarely, under saturating ATP. Every second step occurs at ~12 s^{-1}, intervening steps require much longer periods. The existence of such data suggests that every second step occurs from a similar biochemical state, which is consistent with models predicting that the two heads alternate roles with each unitary advance. The step distance in this data, taken with the dual-bead trapping geometry, is probably compromised by elastic linkages in the system.

its direction of movement (see Coppin et al., 1997), which would counter predictions of the above models? (9) How do Ca^{2+} and the light chains regulate motor activity? Although I have not covered this here, it remains an interesting area of research for this and other myosins. Thus far, we have evidence that Ca^{2+} suppresses motility in myosin V monomers and dimers (Cheney et al., 1993; Trybus et al., 1999; Homma et al., 2000), suppresses (Trybus et al., 1999; Homma et al., 2000), and doesn't affect (Trybus et al., 1999; Wang et al., 2000) ATPase rates in truncated fragments, activates ATPase rates in tissue-purified dimers (Cheney et al., 1993; Nasciamento et al., 1996; Wang et al., 2000) and induces light-chain removal from the neck region (Cheney et al., 1993; Nasciamento et al., 1996; Trybus et al., 1999; Homma et al., 2000). The effects of Ca^{2+} on ATP turnover and motility are likely to be distinct: truncated myosin V monomer and dimer constructs lose motility at a pCa of 6, whereas they release calmodulins and reduce their ATP-turnover rates only at a pCa of 5 (Homma et al., 2000). These provide the opening clues in an interesting mystery. (10) On a related note, does the C-terminal cargo-binding domain affect the motor domain? Might the C-terminal domain be required for processivity? If so, how is such regulation achieved? (11) How does motility correlate with conformational change? For instance, if a rigid stepping intermediate predominates kinetically at some load and ATP conditions, but a floppy intermediate prevails under others, single molecule fluorescence observations (Warshaw et al., 1998), perhaps simultaneous with mechanical measurements (see Ishijima et al., 1998), should reveal these states. A comprehensive understanding will require observation of conformational changes during processive stepping.

Efforts to solve these remaining mysteries will no doubt unearth new puzzles regarding this giant molecular walking machine. The pace of advances in our understanding of myosin V has generated considerable excitement; one observer recently declared that myosin V should "advance rapidly the study of myosin motors and lead it to the final stage" (Yanagida and Iwane, 2000). However imminent this final stage might feel, it seems clear that study of myosin V will remain a vibrant and revealing endeavor for some time to come.

I thank Richard Cheney, Yong Choe, Enrique De La Cruz, William Hancock, Peter Knight, Marcelo Magnasco, Daniel Pierce, Matthias Rief, Ronald Rock, Doug Smith, Taro Uyeda, and Koen Visscher for valuable discussions and comments on the manuscript. I also thank Enrique De La Cruz and Dietmar Manstein for sharing unpublished data. Finally, I thank Enrique De La Cruz for sharing unpublished ideas.

References

Anson, M., Geeves, M. A., Kurzawa, S. E. and Manstein, D. J. (1996). Myosin motors with artificial lever arms. *EMBO J.* **15**, 6069-6074.

Bagshaw, C. (1982). *Muscle Contraction*. London: Champman and Hall.

Berg, O. G. and von Hippel, P. H. (1985). Diffusion-controlled macromolecular interactions. *Annu. Rev. Biophys. Chem.* **14**, 131-160.

Block, S. M., Goldstein, L. S. and Schnapp, B. J. (1990). Bead movement by single kinesin molecules studied with optical tweezers. *Nature* **348**, 348-352.

Byassee, T. A., Chan, W. C. and Nie, S. (2000). Probing single molecules in single living cells. *Anal. Chem.* **72**, 5606-5611.

Burgess, S., Walker, M., Schmitz, S., Wang, F., Seller, J. R., Knight, P. J. and Trinick, J. (2001). Direct visualization of gross conformational changes in the heads of myosin V between different nucleotide states. *Biophys. J.* **80**, 341a

Cheney, R. E., O'Shea, M. K., Heuser, J. E., Coelho, M. V., Wolenski, J. S., Espreafico, E. M., Forscher, P., Larson, R. E. and Mooseker, M. S. (1993). Brain myosin-V is a two-headed unconventional myosin with motor activity. *Cell* **75**, 13-23.

Cheney, R. E. (1998). Purification and assay of myosin-V. *Methods Enzymol.* **298**, 3-18.

Chung, J., Hua, W. and Gelles, J. (2001). Evidence against the kinesin symmetric hand-over-hand model. (2001). *Biophys. J.* **80**, 570a.

Conibear, P. B. and Geeves, M. A. (1998). Cooperativity between the two heads of rabbit skeletal muscle heavy meromyosin in binding to actin. *Biophys. J.* **75**, 926-937.

Coppin, C. M., Pierce, D. W., Hsu, L. and Vale, R. D. (1997). The load dependence of kinesin's mechanical cycle. *Proc. Natl. Acad. Sci. USA* **94**, 8539-8544.

Corrie, J. E. T., Brandmeier, B. D., Ferguson, R. E., Trentham, D. R., Kendrick-Jones, J., Hopkins, S. C., Van der Heide, U. A., Goldman, Y. E., Sabido-David, C., Dale, R. E., Criddle, S. and Irving, M. (1999). Dynamic measurement of myosin light-chain-domain tilt and twist in muscle contraction. *Nature* **200**, 425-430.

Coy, D. L., Wagenbach, M. and Howard, J. (1999a). Kinesin takes one 8-nm step for each ATP that it hydrolyzes. *J. Biol. Chem.* **274**, 3667-3671.

Coy, D. L., Hancock, W. O., Wagenbach, M. and Howard, J. (1999b). Kinesin's tail domain is an inhibitory regulator of the motor domain. *Nat. Cell Biol.* **1**, 288-292.

Cremo, C. R. and Geeves, M. A. (1998). Interaction of actin and ADP with the head domain of smooth muscle myosin: implications for strain-dependent ADP release in smooth muscle. *Biochemistry* **37**, 1969-1978.

Crevel, I., Carter, N., Schliwa, M. and Cross, R. (1999). Coupled chemical and mechanical reaction steps in a processive Neurospora kinesin. *EMBO J.* **18**, 5863-5872.

Dantzig, J. A., Goldman, Y. E., Millar, N. C., Lacktis, J. and Homsher, E. (1992). Reversal of the cross-bridge force-generating transition by photogeneration of phosphate in rabbit psoas muscle fibres. *J. Physiol.* **451**, 247-278.

Davenport, R. J., Wuite, G. J. L., Landick, R. and Bustamante, C. (2000). Single-molecule study of transcriptional pausing and arrest by *E. coli* RNA polymerase. *Science* **287**, 2497-2500.

De La Cruz, E. M., Wells, A. L., Rosenfeld, S. S., Ostap, E. M. and Sweeney, H. L. (1999). The kinetic mechanism of myosin V. *Proc. Natl. Acad. Sci. USA* **96**, 13726-13731.

De La Cruz, E. M., Wells, A. L., Sweeney, H. L. and Ostap, E. M. (2000a). Actin and light chain isoform dependence of myosin V kinetics. *Biochemistry* **39**, 14196-14202.

De La Cruz, E. M., Sweeney, H. L. and Ostap, E. M. (2000b). ADP inhibition of myosin V ATPase activity. *Biophys. J.* **79**, 1524-1529.

Dias, D. P., Whittaker, M., Wells, A. P., Brown, F., Sweeney, H. L. and Milligan, R. A. (1997). Structures of myosin V head in different nucleotide states by cryo-EM and image analysis. *Mol. Biol. Cell* **8S**, 371a.

Dominguez, R., Freyzon, Y., Trybus, K. M. and Cohen, C. (1998). Crystal

structure of a vertebrate smooth muscle myosin motor domain and its complex with the essential light chain: visualization of the pre-power stroke state. *Cell* **94**, 559-571.

Egelman, E. H. and DeRosier, D. J. (1992). Image analysis shows that variations in actin crossover spacings are random, not compensatory. *Biophys. J.* **63**, 1299-1305.

Einstein, A. (1956). *Investigations on the Theory of Brownian Movement* (ed. Furth, R.). New York: Dover.

Ellis, R. J. (2001). Macromolecular crowding: an important but neglected aspect of the intracellular environment. *Curr. Opin. Struct. Biol.* **11**, 114-119.

Espindola, F. S., Suter, D. M., Partata, L. B., Cao, T., Wolenski, J. S., Cheney, R. E., King, S. M. and Mooseker, M. S. (2000). The light chain composition of chicken brain myosin-Va: calmodulin, myosin-II essential light chains, and 8-kDa dynein light chain/PIN. *Cell Motil. Cytoskel.* **47**, 269-281.

Espreafico, E. M., Cheney, R. E., Matteoli, M., Nascimento, A. A., De Camilli, P. V., Larson, R. E. and Mooseker, M. S. (1992). Primary structure and cellular localization of chicken brain myosin-V (p190), an unconventional myosin with calmodulin light chains. *J. Cell Biol.* **119**, 1541-1557.

Evans, L. L., Lee, A. J., Bridgman, P. C. and Mooseker, M. S. (1998). Vesicle-associated brain myosin-V can be activated to catalyze actin-based transport. *J. Cell Sci.* **111**, 2055-2066.

Fenn, W. O. (1924). The relation between the work performed and the energy liberated in muscular contraction. *J. Physiol.* **184**, 373-395.

Finer, J. T., Simmons, R. M. and Spudich, J. A. (1994). Single myosin molecule mechanics: piconewton forces and nanometre steps. *Nature* **368**, 113-119.

Friedman D. S. and Vale, R. D. (1999). Single-molecule analysis of kinesin motility reveals regulation by the cargo-binding tail domain. *Nat. Cell Biol.* **1**, 293-297.

Funatsu, T., Harada, Y., Tokunaga, M., Saito, K. and Yanagida, T. (1995). Imaging of single fluorescent molecules and individual ATP turnovers by single myosin molecules in aqueous solution. *Nature* **374**, 555-559.

Geeves, M. A., Perreault-Micale, C. and Coluccio, L. M. (2000). Kinetic analyses of a truncated mammalian myosin I suggest a novel isomerization event preceding nucleotide binding. *J. Biol. Chem.* **275**, 21624-21630.

Gilbert, S. P., Webb, M. R., Brune, M. and Johnson, K. A. (1995). Pathway of processive ATP hydrolysis by kinesin. *Nature* **373**, 671-676.

Gilbert, S. P., Moyer, M. L. and Johnson, K. A. (1998). Alternating site mechanism of the kinesin ATPase. *Biochemistry* **37**, 792-799.

Gittes, F., Meyhofer, E., Baek, S. and Howard, J. (1996). Directional loading of the kinesin motor as it buckles a microtubule. *Biophys. J.* **70**, 418-429.

Hackney, D. D. (1994). Evidence for alternating head catalysis by kinesin during microtubule-stimulated ATP hydrolysis. *Proc. Natl. Acad. Sci. USA* **91**, 6865-6869.

Hackney, D. D. (1995). Highly processive microtubule-stimulated ATP hydrolysis by dimeric kinesin head domains. *Nature* **377**, 448-450.

Hackney, D. D. and Clark, P. K. (1984). Catalytic consequences of oligomeric organization: kinetic evidence for "tethered" acto-heavy meromyosin at low ATP concentrations. *Proc. Natl. Acad. Sci. USA* **17**, 5345-5349.

Hackney, D. D. and Stock, M. F. (2000). Kinesin's IAK tail domain inhibits initial microtubule-stimulated ADP release. *Nat. Cell Biol.* **2**, 257-260.

Hackney, D. D., Levitt, J. D., and Suhan, J. (1992). Kinesin undergoes a 9 S to 6 S conformational transition. *J. Biol. Chem.* **267**, 8696-8701.

Hancock, W. O. and Howard, J. (1998). Processivity of the motor protein kinesin requires two heads. *J. Cell Biol.* **140**, 1395-1405.

Hancock, W. O. and Howard, J. (1999). Kinesin's processivity results from mechanical and chemical coordination between the ATP hydrolysis cycles of the two motor domains. *Proc. Natl. Acad. Sci. USA* **23**, 13147-13152.

Harada, Y., Noguchi, A., Kishino, A. and Yanagida, T. (1987). Sliding movement of single actin filaments on one-headed myosin filaments. *Nature* **326**, 805-808.

Hibberd, M. G. and Trentham, D. R. (1986). Relationships between chemical and mechanical events during muscular contraction. *Annu. Rev. Biophys. Chem.* **15**, 119-161.

Hirokawa, N. (1982). Cross-linker system between neurofilaments, microtubules, and membranous organelles in frog axons revealed by the quick-freeze, deep-etching method. *J. Cell Biol.* **94**, 129-142.

Homma, K., Saito, J., Ikege, R. and Ikege, M. (2000). Ca^{2+}-dependent regulation of the motor activity of myosin V. *J. Biol. Chem.* **275**, 34766-34771.

Howard, J. (1995). The mechanics of force generation by kinesin. *Biophys. J.* **68**, Suppl. 245-255.

Howard, J. (1997). Molecular motors: structural adaptations to cellular functions. *Nature* **389**, 561-567.

Howard, J., Hudspeth, A. J. and Vale, R. D. (1989). Movement of microtubules by single kinesin molecules. *Nature* **342**, 154-158.

Hua, W., Young, E. C., Fleming, M. L. and Gelles, J. (1997). Coupling of kinesin steps to ATP hydrolysis. *Nature* **388**, 390-393.

Hua, W., Chung, J and Gelles, J. (2001). Kinesin does not rotate during stepping. *Biophys. J.* **80**, 512a.

Huang, J. D., Brady, S. T., Richards, B. W., Stenoien, D., Resau, J. H., Copeland, N. G. and Jenkins, N. A. (1999). Direct interaction of microtubule- and actin-based transport motors. *Nature* **397**, 267-270.

Huxley, A. F. (1957). Muscle structure and theories of contraction. *Prog. Biophys. Biophys. Chem.* **7**, 255-318.

Hunt, A. J. and Howard, J. (1993). Kinesin swivels to permit microtubule movement in any direction. *Proc. Natl. Acad. Sci. USA* **90**, 11653-11657.

Hunt, A. J., Gittes, F. and Howard, J. (1994). The force exerted by a single kinesin molecule against a viscous load. *Biophys. J.* **67**, 766-781.

Ishii, Y. and Yanagida, T. (2000). Single molecule detection in Life Science. *Single Mol.* **1**, 5-16.

Ishijima, A., Kojima, H., Funatsu, T., Tokunaga, M., Higuchi, H., Tanaka, H. and Yanagida, T. (1998). Simultaneous observation of individual ATPase and mechanical events by a single myosin molecule during interaction with actin. *Cell* **92**, 161-171.

Ito, K., Liu, X., Katayama, E. and Uyeda, T. Q. (1999). Cooperativity between two heads of dictyostelium myosin II in in vitro motility and ATP hydrolysis. *Biophys. J.* **76**, 985-992.

Iwatani, S., Iwane, A. H., Higuchi, H., Ishi, Y. and Yanagida, T. (1999). Mechanical and chemical properties of cysteine-modified kinesin molecules. *Biochemistry* **38**, 10318-10323.

Johnson, K. A. and Taylor, E. W. (1978). Intermediate states of subfragment 1 and actosubfragment 1 ATPase: reevaluation of the mechanism. *Biochemistry* **17**, 3432-3442.

Jontes, J. D., Milligan, R. A., Pollard, T. D. and Ostep, E. M. (1997). Kinetic characterization of brush border myosin-I ATPase. *Proc. Natl. Acad. Sci. USA* **94**, 14332-14337.

Kitamura, K., Tokunaga, M., Iwane, A. H. and Yanagida, T. (1999). A single myosin head moves along an actin filament with regular steps of 5.3 nanometres. *Nature* **397**, 129-134.

Kojima, H., Muto, E., Higuchi, H. and Yanagida, T. (1997). Mechanics of single kinesin molecules measured by optical trapping nanometry. *Biophys. J.* **73**, 2012-2022.

Kron, S. J. and Spudich, J. A. (1986). Fluorescent actin filaments move on myosin fixed to a glass surface. *Proc. Natl. Acad. Sci. USA* **83**, 6272-6276.

Kuo, S. C. and Sheetz, M. P. (1993). Force of single kinesin molecules measured with optical tweezers. *Science* **260**, 232-234.

Landau, L. D. and Lifshitz, E. M. (1980). *Statistical Physics*. Oxford: Pergamon Press.

Lang, M. F., Asbury, C. L., Shaevitz, J. W. and Block, S. M. (2001). A 2D force clamp for kinesin with fluorescence capability. *Biophys. J.* **80**, 571a.

Leibler, S. and Huse, D. A. (1993). Porters versus rowers: a unified stochastic model of motor proteins. *J. Cell Biol.* **121**, 1357-1368.

Lohman, T. M., Thorn, K. and Vale, R. D. (1998). Staying on track: common features of DNA helicases and microtubule motors. *Cell* **92**, 9-12.

Ma, Y. and Taylor, E. W. (1997). Interacting head mechanism of microtubule-kinesin ATPase. *J. Biol. Chem.* **272**, 724-730.

Maier, B., Bensimon, D. and Croquette, V. (2000). Replication by a single DNA polymerase of a stretched single-stranded DNA. *Proc. Natl. Acad. Sci. USA* **97**, 12002-12007.

Mehta, A. D., Finer, J. T. and Spudich, J. A. (1998). Use of optical traps in single-molecule study of non-processive biological motors. *Methods Enzymol.* **298**, 436-459.

Mehta, A. D., Rock, R. S., Rief, M., Spudich, J. A., Mooseker, M. S. and Cheney, R. E. (1999a). Myosin-V is a processive actin-based motor. *Nature* **400**, 590-593.

Mehta, A. D., Rief, M., Spudich, J. A., Smith, D. A. and Simmons, R. M. (1999b). Single-molecule biomechanics with optical methods. *Science* **283**, 1689-1695.

Mermall, V., Post, P. L. and Mooseker, M. S. (1998). Unconventional myosins in cell movement, membrane traffic and signal transduction. *Science* **279**, 527-533.

Meyhofer, E. and Howard, J. (1995). The force generated by a single

kinesin molecule against an elastic load. *Proc. Natl. Acad. Sci. USA* **92**, 574-578.

Miller, K. E. and Sheetz, M. P. (2000). Characterization of myosin V binding to brain vesicles. *J. Biol. Chem.* **275**, 2598-2606.

Molloy, J. E., Kendrick-Jones, J., Veigel, C. and Tregear, R. T. (2000). An unexpectedly large working stroke from chymotryptic fragments of myosin II. *FEBS Lett.* **480**, 293-297.

Moore, J. R., Krementsova, E., Trybus, K. M. and Warshaw, D. M. (2000). Myosin V exhibits a high duty cycle and large unitary displacement at zero load. *Biophys. J.* **78**, 272a.

Moore, J. R., Krementsova, E., Trybus, K. M. and Warshaw, D. M. (2001). Molecular mechanisms of expressed myosin V. *Biophys. J.* **80**, 574a.

Murphy, C. T. and Spudich, J. A. (2000). Variable surface loops and myosin activity: accessories to a motor. *J. Muscle Res. Cell Motil.* **21**, 139-151.

Nascimento, A. A. C., Cheney, R. E., Tauhata, S. B. F., Larson, R. E. and Mooseker, M. S. (1996). Enzymatic characterization and functional domain mapping of brain myosin-V. *J. Biol. Chem.* **271**, 17561-17569.

Okada, Y. and Hirokawa, N. (1999). A processive single-headed motor: kinesin superfamily protein KIF1A. *Science* **283**, 1152-1157.

Okada, Y. and Hirokawa, N. (2000). Mechanism of the single-headed processivity: diffusional anchoring between the K-loop of kinesin and the C terminus of tubulin. *Proc. Natl. Acad. Sci. USA* **97**, 640-645.

Perkins, T. T., Mitsis, P. G., Dalal, R. V. and Block, S. M. (2001). Watching enzymes move along DNA one at a time. *Biophys. J.* **80**, 349a.

Provance, D. W., Jr and Mercer, J. A. (1999). Myosin V: head to tail *Cell. Mol. Life Sci.* **56**, 233-242.

Pollard, T. D. (2000). Reflections on a quarter century of research on contractile systems. *Trends Biochem. Sci.* **25**, 607-611.

Reck-Peterson, S. L., Novick, P. J. and Mooseker, M. S. (1999). The tail of a yeast class V myosin, myo2p, functions as a localization domain. *Mol. Biol. Cell* **10**, 1001-1017.

Reck-Peterson, S. L., Provance, D. W., Jr, Mooseker, M. S. and Mercer, J. A. (2000a). Class V myosins. *Biochim. Biophys. Acta* **1496**, 36-51.

Reck-Peterson, S. L., Tyska, M. J., Novick, P. J. and Mooseker, M. S. (2000b). The yeast class V myosins, Myo2p and Myo4p, are non-processive actin-based motors. *Mol. Biol. Cell* **11**, 373a.

Rice, S., Lin, A. W., Safer, D., Hart, C. L., Naber, N., Carragher, B. O., Cain, S. M., Pechatnikova, E., Wilson-Kubalek, E. M., Whittaker, M. et al. (1999). A structural change in the kinesin motor protein that drives motility. *Nature* **402**, 778-784.

Rief, M., Rock, R. S., Mehta, A. D., Mooseker, M. S., Cheney, R. E. and Spudich, J. A. (2000). Myosin V stepping kinetics: a molecular model for processivity. *Proc. Natl. Acad. Sci. USA* **97**, 9482-9486.

Rock, R. S., Rief, M., Mehta, A. D. and Spudich, J. A. (2000). In vitro assays of processive myosin motors. *Methods Enzymol.* (in press).

Rogers, S. L. and Gelfand, V. (1998). Myosin cooperates with microtubule motors during organelle transport in melanophores. *Curr. Biol.* **8**, 161-164.

Romberg, L., Pierce, D. W. and Vale, R. D. (1998). Role of the kinesin neck region in processive microtubule-based motility. *J. Cell Biol.* **140**, 1407-1416.

Rosenfeld, S. S., Xing, J., Whitaker, M., Cheung, H. C., Brown, F., Wells, A., Milligan, R. A. and Sweeney, H. L. (2000). Kinetic and spectroscopic evidence for three actomyosin: ADP states in smooth muscle. *J. Biol. Chem.* **275**, 25418-25426.

Ruff, C., Furch, M., Brenner, B., Manstein, D. J. and Meyhofer, E. (2001). Single-molecule tracking of myosins with genetically engineered amplifier domains. *Nat. Struct. Biol.* **8**, 226-229.

Sakakibara, H., Kojima, H., Sakai, Y., Katayama, E. and Oiwa, K. (1999). Inner-arm dynein c of Chlamydomonas flagella is a single-headed processive motor. *Nature* **400**, 586-590.

Sakamoto, T., Amitani, I., Yokota, E. and Ando, T. (2000). Direct observation of processive movement by individual myosin V molecules. *Biochem. Biophys. Res. Commun.* **272**, 586-590.

Schief, W. R. and Howard, J. (2001). Conformational changes during kinesin motility. *Curr. Opin. Cell Biol.* **13**, 19-28.

Schnitzer, M. J. and Block, S. M. (1995). Statistical kinetics of processive enzymes. *Cold Spring Harbor Symp. Quant. Biol.* **60**, 793-802.

Schnitzer, M. J. and Block, S. M. (1997). Kinesin hydrolyses one ATP per 8-nm step *Nature* **388**, 386-390.

Schnitzer, M. J., Visscher, K. and Block, S. M. (2000). Force production by single kinesin motors *Nat. Cell Biol.* **2**, 718-723.

Shih, W., Gryczynski, Z., Lakowicz, J. R. and Spudich, J. A. (2000). A FRET-based sensor reveals ATP hydrolysis dependent large conformational changes and three distinct states of the molecular motor myosin. *Cell* **102**, 683-694.

Spudich, J. A. (1994). How molecular motors work. *Nature* **372**, 515-518.

Suzuki, Y., Yasunaga, T., Ohkura, R., Wakabayashi, T. and Sutoh, K. (1998). Swing of the lever arm of a myosin motor at the isomerization and phosphate-release steps. *Nature* **396**, 380-383.

Svoboda, K., Schmidt, C. F., Schnapp, B. J. and Block, S. M. (1993). Direct observation of kinesin stepping by optical trapping interferometry. *Nature* **365**, 721-727.

Svoboda, K. and Block, S. M. (1994). Force and velocity measured for single kinesin molecules. *Cell* **77**, 773-784.

Svoboda, K., Mitra, P. P. and Block, S. M. (1994). Fluctuation analysis of motor protein movement and single enzyme kinetics. *Proc. Natl. Acad. Sci. USA* **91**, 11782-11786.

Tanaka, H., Ishijima, A., Honda, M., Saito, K. and Yanagida, T. (1998). Orientation dependence of displacements by a single one-headed myosin relative to the actin filament. *Biophys. J.* **75**, 1886-1894.

Tanaka, H., Iwane, A. H. and Yanagida, T. (2000). Role of the myosin neck region in generation of movement. *Biophys. J.* **78**, 234a.

Tanaka, H., Homma, K., Iwane, A. H., Katayama, E., Ikebe, R., Saito, J., Yanagida, T. and Ikebe, M. (2001). The motor domain, not a long neck domain, determines the large step of myosin V. *Biophys. J.* **80**, 81a.

Tans, S., Smith, D., Smith, S., Grimes, S., Anderson, D. and Bustamante, C. (2001). Single molecule studies of the DNA packaging motor of bacteriophage ϕ29. *Biophys. J.* **80**, 200a.

Titus, M. A. (1997). Myosin V - the multi-purpose transport motor. *Curr. Biol.* **7**, 301-304.

Trybus, K. M., Krementsova, E. and Freyzon, Y. (1999). Kinetic characterization of a monomeric unconventional myosin V construct. *J. Biol. Chem.* **274**, 27448-27456.

Tyska, M. J., Dupuis, D. E., Guilford, W. H., Patlak, J. B., Waller, G. S., Trybus, K. M., Warshaw, D. M. and Lowey, S. (1999). Two heads of myosin are better than one for generating force and motion. *Proc. Natl. Acad. Sci. USA* **96**, 4402-4407.

Uyeda, T. Q., Kron, S. J. and Spudich, J. A. (1990). Myosin step size estimation from slow sliding movement of actin over low densities of heavy meromyosin. *J. Mol. Biol.* **214**, 699-710.

Uyeda, T. Q., Warrick, H. M., Kron, S. J. and Spudich, J. A. (1991). Quantized velocities at low myosin densities in an in vitro motility assay. *Nature* **352**, 307-311.

Uyeda, T. Q., Abramson, P. D. and Spudich, J. A. (1996). The neck region of the myosin motor domain acts as a lever arm to generate movement. *Proc. Natl. Acad. Sci. USA* **93**, 4459-4464.

Uyeda, T. Q., Katayama, E., Kaseda, K., Tokuraku, K. and Patterson, B. (2001). An extended prestroke A.S1.ADP.Pi state of G680V mutant dictyostelium S1 in the presence of ATP. *Biophys. J.* **80**, 81a.

Vale, R. D., Funatsu, T., Pierce, D. W., Romberg, L., Harada, Y. and Yanagida, T. (1996). Direct observation of single kinesin molecules moving along microtubules. *Nature* **380**, 451-453.

Vale, R. D. and Milligan, R. A. (2000). The way things move: looking under the hood of molecular motor proteins. *Science* **288**, 88-95.

Veigel, C., Wang, F., Bartoo, M. L., Hammer, J., Sellers, J. R. and Molloy, J. E. (2001). Mechanical properties of single myosin V molecules. *Biophys. J.* **80**, 199a.

Visscher, K. and Block, S. M. (1998). Versatile optical traps with feedback control. *Methods Enzymol.* **298**, 460-489.

Visscher, K., Schnitzer, M. J. and Block, S. M. (1999). Single kinesin molecules studied with a molecular force clamp. *Nature* **400**, 184-189.

Walker, M. L., Burgess, S. A., Sellers, J. R., Wang, F., Hammer, J. A., III, Trinick, J. and Knight, P. J. (2000). Two-headed binding of a processive myosin to F-actin. *Nature* **405**, 804-807.

Wang, F., Chen, L., Arcucci, O., Harvey, E. V., Bowers, B., Xu, Y., Hammer, J. A., III and Sellers, J. R. (2000). Effect of ADP and ionic strength on the kinetic and motile properties of recombinant mouse myosin V. *J. Biol. Chem.* **275**, 4329-4335.

Wang, M. D., Schnitzer, M. J., Yin, H., Landick, R., Gelles, J. and Block, S. M. (1998). Force and velocity measured for single molecules of RNA polymerase. *Science* **282**, 902-907.

Warshaw, D. M., Hayes, E., Gaffney, D., Lauzon, A., Wu, J., Kennedy, G., Trybus, K., Lowey, S. and Berger, C. (1998). Myosin conformational states determined by single fluorophore polarization. *Proc. Natl. Acad. Sci. USA* **95**, 8034-8039.

Warshaw, D. M., Guilford, W. H., Freyzon, Y., Krementsova, E., Palmiter, K. A., Tyska, M. J., Baker, J. and Trybus, K. M. (2000). The light chain

binding domain of expressed s*mooth* muscle heavy meromyosin acts as a mechanical lever. *J. Biol. Chem.* **275**, 37167-37172.

Wolenski J. S., Cheney R. E., Mooseker M. S. and Forscher P. (1995). In vitro motility of immunoadsorbed brain myosin-V using a Limulus acrosomal process and optical tweezer-based assay. *J. Cell Sci.* **108**, 1489-1496.

Wu, X., Bowers, B., Rao, K., Wei, Q. and Hammer, J. A. (1998). Visualization of melanosome dynamics within wild-type and dilute melanocytes suggests a paradigm for myosin-V function in vivo. *J. Cell Biol*. **143**, 1899-1918.

Wuite, G. J. L., Smith, S. B., Young, M., Keller, D. and Bustamante, C. (2000). Single-molecule studies on the effect of template tension on T7 DNA polymerase activity. *Nature* **404**, 103-106.

Yanagida, T., Arata, T. and Oosawa, F. (1985). Sliding distance of actin filament induced by a myosin crossbridge during one ATP hydrolysis cycle. *Nature* **316**, 366-369.

Yanagida, T., Kitamura, K., Tanaka, H., Iwane, A. H. and Esaki, S. (2000). Single-motor mechanics and models of the myosin motor. *Curr. Opin. Cell Biol*. **12**, 20-25.

Yanagida, T. and Iwane, A. H. (2000). A large step for myosin. *Proc. Natl. Acad. Sci. USA* **97**, 9357-9359.